SECTION 5

REVIEW OF VARIABLES AFFECTING CATCHBASIN EFFICIENCY

The principal variables that affect the performance of catchbasins in removing pollutants found in stormwater are reviewed in this section. These variables deal with (1) catchbasin hydrology, (2) catchbasin hydraulics, (3) pollutant characteristics, and (4) solids washoff.

CATCHBASIN HYDROLOGY

The hydrology of the drainage area tributary to the catchbasin is important because the area contributes runoff water to the catchbasin and thus affects the solids loading of the catchbasin. The amount of runoff is controlled by the terrain and street slopes, drainage area size and shape, distance to the catchbasin, runoff coefficients, distribution of pervious and impervious surfaces, lag time, storm intensity and duration, depression and gutter storage, flow routing, and infiltration capacity.

Defining a typical runoff area hyetograph and hydrograph for universal application as an evaluation criterion for catchbasins may be unrealistic. To illustrate this, the variation of localized rainfall intensity extrapolated from the 1963 U.S. Weather Bureau Rainfall-Frequency Atlas for various design storms for three U.S. cities is reported in Table 8. It is apparent that, to be realistic, evaluation should be based on known hydrological data in a known runoff area.

TABLE 8. TYPICAL 5-MINUTE RAINFALL INTENSITIES [106]

Recurrence interval, yr	Intensity, in./h		
	San Francisco	Chicago	Washington, D.C.
10	4.29 (3.1)	8.15 (7.1)	9.94 (7.34)
5	3.48 (2.6)	6.63 (6.1)	8.07 (6.4)
2	2.68 (2.0)	5.10 (4.6)	6.21 (5.25)
1	2.01 (0.9)	3.83 (...)	4.66 (....)

Note: Figures in parenthesis represent official gage data.

cm/h = in./h x 2.54

The area tributary to an inlet is usually dependent on the inlet spacing. For a given rainfall intensity, inlet spacing is dependent primarily on the longitudinal slope of the gutter and the allowable spread of water on the traveled way. Using the typical city street cross-section shown in Figure 6 and assuming a maximum allowable water spread of 182.9 cm (6 ft), excluding 33.5 cm (1.1 ft) of gutter width, the depth of flow at the curb would be 8.2 cm (0.27 ft). Based on the curb depth of 8.2 cm, the maximum flows and corresponding velocities for various longitudinal gutter slopes are shown in Table 9, as computed by using a modified form of Manning's equation [68]:

$$Q = 0.56\ (Z/n)\ S_o^{1/2}\ d^{8/3} \tag{1}$$

where Q = rate of discharge, cfs
Z = reciprocal of the gutter cross slope (T/d)
n = Manning's coefficient of channel roughness
S_o = longitudinal slope, ft/ft
T = top width of water surface, ft
d = depth of channel at deepest point, ft

The true Manning equation cannot be used without modification to compute flow in triangular gutter sections because the hydraulic radius does not adequately describe the gutter cross-section, particularly when the top width T of water surface may be more than 40 times the depth d at the curb. To compute gutter flow, the Manning equation for an increment of width is integrated across the width T using Equation 1. Equation 1 ignores the resistance of the curb face, but this resistance is negligible from a practical viewpoint, provided that the width of flow is at least 10 times the depth at the curb face. Equation 1 gives a discharge about 19 percent greater than the incorrect solution, obtained by computing the discharge by the true Manning equation.

TABLE 9. TYPICAL MAXIMUM GUTTER FLOWS ON OLDER CITY STREETS

Longitudinal gutter slope, m/m	Q, L/s (cfs)	V, cm/s (ft/s)
0.002	25.2 (0.89)	36.6 (1.20)
0.004 (practical minimum)	35.7 (1.26)	51.8 (1.70)
0.010	56.6 (2.0)	82.3 (2.70)
0.060	138.8 (4.9)	201.8 (6.62)
0.100 (practical maximum)	179.0 (6.32)	260.3 (8.54)

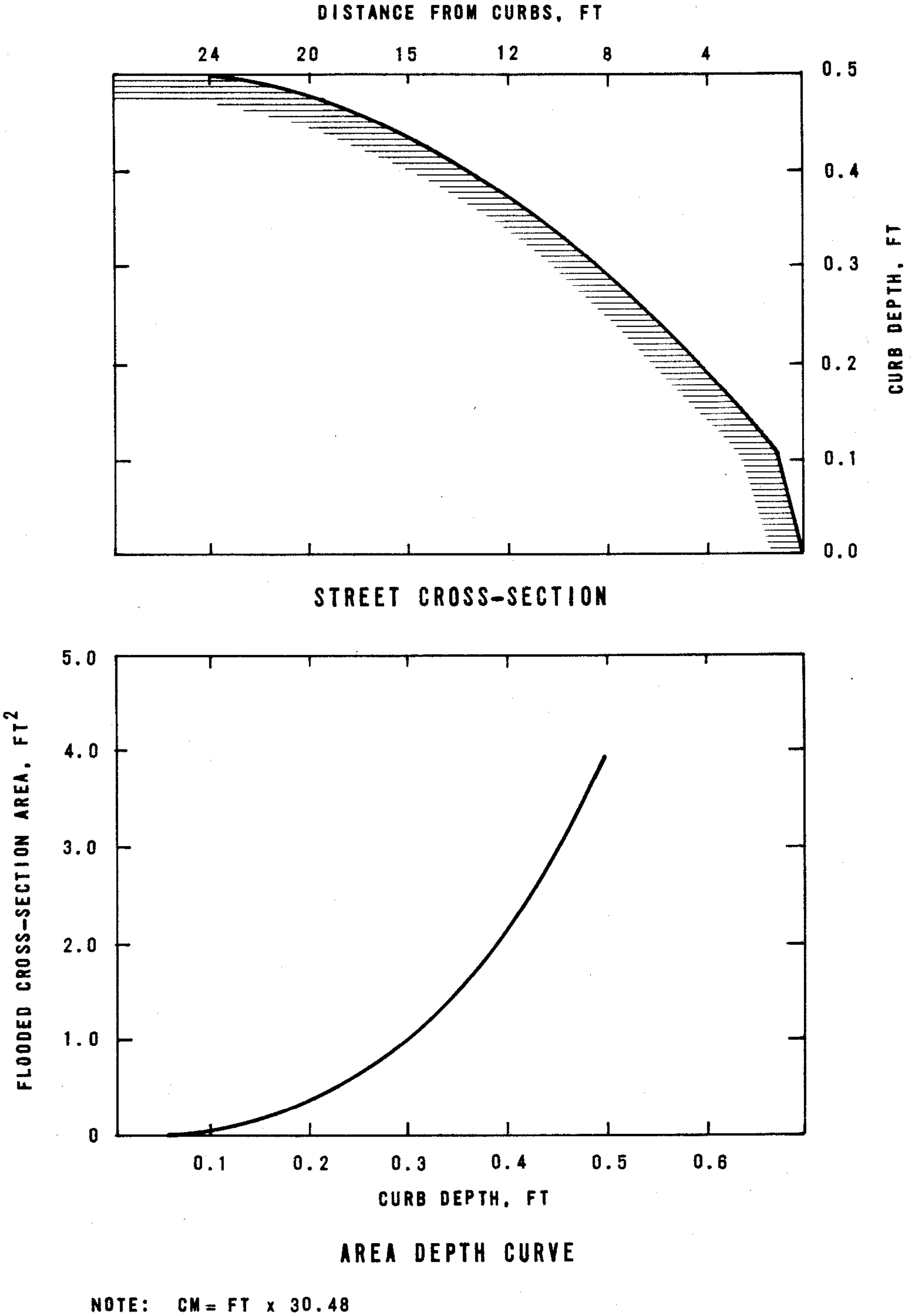

Figure 6. Typical old street cross-section [68].

The corresponding tributary paved areas for the cities in Table 8 can be determined using the Rational formula,

$$Q = CiA \tag{2}$$

where Q = maximum rate of runoff, cfs
C = runoff coefficient = 0.8 to 0.9 for common pavements
i = rainfall intensity corresponding to time of concentration, generally taken as 5 minutes
A = area tributary to inlet, acres

Assuming a 5-year 5-minute storm intensity and a C value of 0.9, tributary paved areas are as given in Table 10. The importance of knowing the tributary area is that the pollutant load entering a catchbasin is directly related. The nature of this relationship is considered in a subsequent subsection.

TABLE 10. TYPICAL TRIBUTARY PAVED AREAS TO CATCHBASINS

Longitudinal gutter slope, m/m	Area, acres		
	San Francisco	Chicago	Washington, D.C.
0.002	0.28 (0.74)	0.15 (0.77)	0.13 (0.41)
0.004	0.40 (1.05)	0.21 (1.08)	0.17 (0.53)
0.010	0.64 (1.68)	0.34 (1.74)	0.28 (0.88)
0.060	1.56 (4.11)	0.82 (4.20)	0.67 (2.09)
0.100	2.02 (5.31)	1.06 (5.44)	0.87 (2.72)

Note: Figures in parenthesis indicate approximate total tributary area, both paved and unpaved, to a catchbasin [84, 42, 80].

ha = acres x 0.40

CATCHBASIN HYDRAULICS

The hydraulics of a catchbasin are defined and determined by the geometric configuration. The standard basin is basically a barrel 182.9 cm (6 ft) deep and 121.9 cm (4 ft) in diameter with an open top covered by a grating and an outlet pipe mounted at the side approximately 107 cm (3-1/2 ft) above the bottom. The hydraulics of such a system are best defined by following the flow from the top entrance through the intermittent storage in the barrel to the outflow through the pipe outlet.

The entrance flow conditions vary from a simple drop inlet condition to free surface, peripheral, weir-type overflow to orifice flow entering a barrel. Obviously, the inflow pattern is modified by the grating, which tends to spread the flow over the top and to direct the flow in the form of jets falling between the grating bars. The approach flow conditions also play an important role, especially if there is a considerable approach velocity. With a diminishing velocity of approach, the inflow into the catchbasin is more uniform, and the discharge into the catchbasin is more uniform and more concentrated around the periphery. Comparative data on the intake capacities of various inlets are given in Figure 7.

The flow in the barrel of the catchbasin consists first of filling the basin until the water surface reaches the invert of the outlet pipe, at which time a control of outflow is established. Depending on the slope of the pipe and entrance geometry, a discharge control is effected. Under these conditions, two controls exist, and the flow through the basin presents a miniature flood-routing phenomenon of inflow from the top, temporary storage in the basin, and controlled outflow into the outlet pipe.

The control at the outlet pipe is typical of discharge characteristics through a closed conduit, generally defined in hydraulics as culvert flow. Different regimes can be established for such a flow, beginning with weir control, proceeding to orifice control, and finally reaching full pipe flow. Once the opening becomes submerged, the discharge capacity diminishes (discharge to square root of head relationship for pressure flow, as contrasted to discharges to headwater to 3/2 power relationship for open channel flow). If the outlet end is submerged, the capacity will depend on the hydraulic gradient between the head in the barrel and the head at the end of the outlet pipe.

When the flow in the outlet pipe becomes pressure flow and the catchbasin is full, the head differential between the surface on the street and pressure gradient in the main sewer conduit determines the flow conveyance and discharge. The two controls merge into one, and the geometric configurations of the barrel and the entrance into the pipe outlet become important only in terms of the coefficient for minor losses.

<u>Influence of Various Parameters on Hydraulics</u>

The key parameters in controlling the flow through the basin are the geometric configuration of the top entrance (see Figure 7), the volumetric capacity of the catchbasin, and the elevation, slope, and entrance geometry of the outlet conduit. By properly changing these variables, the catchbasin system can be optimized to make it hydraulically most efficient for whatever purposes are intended.

CURVE ① CURB OPENING, NO DEPRESSION, GRATE LENGTH, L = 10 FT
CURVE ② CURB OPENING, 2½-IN. DEPRESSION, L=10 FT
CURVE ③ CURB OPENING, 3-FT WIDE DEFLECTOR, L=8.33 FT
CURVE ④ GRATE, NO DEPRESSION, W=2.5 FT, L=2.5 FT
CURVE ⑤ GRATE, 2½-IN. DEPRESSION, W=2.5 FT, L=2.5 FT
CURVE ⑥ COMBINATION, NO DEPRESSION
CURVE ⑦ COMBINATION, 2½-IN. DEPRESSION

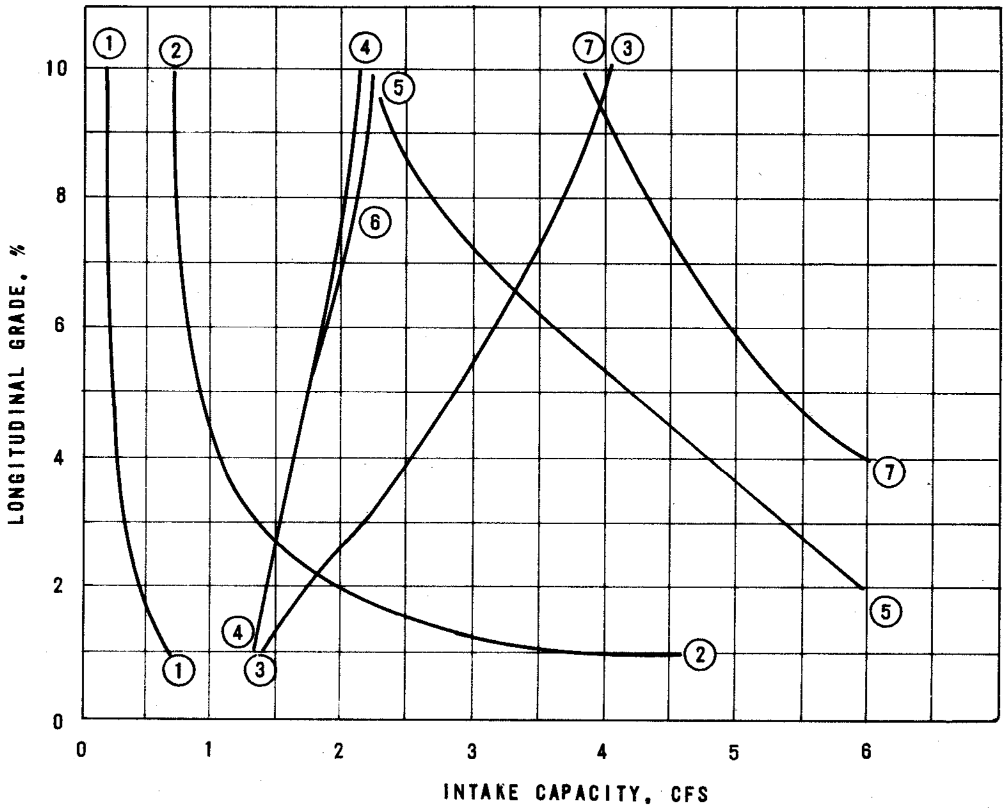

NOTE: CM = FT x 30.48

Figure 7. Comparison of inlets: intake capacity at 95% capture of gutter flow: Manning's n = 0.013; cross slope = 0.0417 ft/ft [76].

Control of the Flow of Solids

Control of the solids flow by an intentional retention or sluicing of solid material through the catchbasin can be effected by modifications in catchbasin geometry. Establishing a controlled conveyance and detention of flow, such a design can be developed by experimental means. By use of baffles, separate compartments, or flow-controlled devices (like weirs, orifices, or side weirs), a flow conveyance can be established so that the flow pattern is effective for whatever action is intended in the movement of solid material. The consideration of turbulence, flow agitation, and other conditions plays an important part in proper development of the necessary geometry.

Other methods for the conveyance or separation of solid material include swirl chambers, spiral flow, flow around bends, and other ways of exploiting some definite hydraulic characteristics.

POLLUTANT CHARACTERISTICS

Pollutants in stormwater can be divided into the four general categories of floatable, dissolved, suspended, and settleable material. Each category can be further subdivided into organic and inorganic components.

Because this report is concerned primarily with catchbasin performance, the pollutant sources of interest are limited to street accumulations and to those pollutants generated in catchbasins. Stormwater pollutants are of concern only for gross comparisons, because collected stormwater contains pollutants from other sources as well as catchbasins. Unfortunately, these limitations also greatly reduce the amount of available data. Although many studies have been performed on stormwater after collection (for example, in combined or storm sewers), few studies have been performed on catchbasin pollutants.

From a recent study that dealt principally with street surface contaminants on a nationwide basis, the following applicable conclusions were formed [66].

1. Runoff from street surfaces is generally highly contaminated.

2. The major constituent of street surface contaminants is inorganic, mineral-like matter, similar to common sand and silt.

3. A great portion of the overall pollutional potential is associated with the fine solids fraction of the street surface contaminants.

4. On the basis of specially conducted field studies, catchbasins (as they are normally used) are reasonably effective in removing coarse inorganic solids from storm runoff (coarse sand and gravel) but ineffective in removing fine solids and most organic matter.

Little information is available on the floatable portion or the dissolved portion of street contaminants. However, the suspended and settleable solids portion of street surface contaminants has been studied with respect to particle size and distribution and the distribution of organic, inorganic, and specific pollutants [66]. The following qualifications justify consideration of the suspended solids portion only:

1. The dissolved portion of runoff passes on into the storm or combined sewer regardless of the type of intermediate device, whether it is a catchbasin or inlet. The relationship that may exist between dissolved solids generated by street cleaning practices and those occurring naturally has not been studied.

2. The floatable portion is almost impossible to characterize, as it varies from oil droplets to small beach balls and does not seem to be a function of land use classification. The only apparent quantity trait for large floatables deposited on the street surface is their proportionality to street cleaning practices.

3. In one study it was found that an average of 92 percent (by weight) of the *in situ* street litter collected in the sampling program passed through a 2,000 micron screen (10 mesh) and was composed mainly of dust, dirt, sand, and gravel [66].

Particle Size and Distribution

In a recently completed nationwide study of street surface contaminants [66], the contaminants usually found on typical American streets were characterized with respect to particle size; distributions for five cities are reported in Table 11. Street solids loading by land use and as a function of the distance from the curb are given in Table 12.

Using the data derived in this study, a street surface particle size distribution simulant was developed for use in experimental studies, as shown in Table 13.

TABLE 11. PARTICLE SIZE DISTRIBUTION OF SOLIDS, SELECTED CITY COMPOSITES [66]

Particle size ranges	Milwaukee	Bucyrus	Baltimore	Atlanta	Tulsa
Distribution, %[a]					
>4,800 μ	12.0	....	17.4	....	.....
2,000-4,800 μ	12.1	10.1	4.6	14.8	37.1
840-2,000 μ	40.8	7.3	6.0	6.6	9.4
246-840 μ	20.4	20.9	22.3	30.9	16.7
104-246 μ	5.5	15.5	20.3	29.5	17.1
43-104 μ	1.3	20.3	11.5	10.1	12.0
30-43 μ	4.2	13.3	10.1	5.1	3.7
14-30 μ	2.0	7.9	4.4	1.8	3.0
4-14 μ	1.2	4.7	2.6	0.9	0.9
<4 μ	0.5	....	0.9	0.3	0.1
Sand, %					
43-4,800 μ	92.1	74.1	82.1	91.9	92.3
Silt, %					
4-43 μ	7.4	25.9	17.1	7.8	7.6
Clay, %					
<4 μ	0.5	....	0.9	0.3	0.1
Sand, kg/curb km (lb/curb mi)	699 (2,480)	288 (1,020)	238 (845)	111 (394)	85 (300)
Silt, kg/curb km (lb/curb mi)	56 (200)	100 (356)	50 (176)	9.5 (33.5)	8.5 (30)
Clay, kg/curb km (lb/curb mi)	3.8 (13.5)	....	2.6 (9.3)	0.4 (1.3)	0.1 (0.3)

Note: μ = microns.

a. By weight unless otherwise noted.

TABLE 12. STREET SOLIDS LOADING BY LAND USE [66]

Use	Quantity, kg/curb km (lb/curb mi)	Range, kg/curb km (lb/curb mi)	
Residential	338 (1,200)	9-1,946	(31-6,900)
Industrial	790 (2,800)	68-3,384	(240-12,000)
Commercial	102 (360)	17-338	(60-1,200)
Mean value	395 (1,400)	....	....

Street location, distance from curb, cm (in.)	Solids loading intensity, % of total
0-15.2 (0-6)	78
15.2-30.5 (6-12)	10
30.5-101.6 (12-40)	9
101.6-243.8 (40-96)	1
243.8 (96) to centerline	2

TABLE 13. STREET SURFACE SIMULANT [66]

Particle size, μ	Composition, % by weight	Description[a]
2,000	8	Very coarse sand
840-2,000	20	Coarse sand
246-840	30	Medium sand
104-246	20	Fine sand
43-104	16	Very fine sand
43	6	Coarse silt

a. Handbook of Applied Hydrology.

Organic and Inorganic Pollutants

The quantities of various pollutants found on street surfaces are summarized on a weighted mean basis in Table 14. The distribution of various pollutants associated with a particle size range is presented in Table 15. As can be seen, the very fine silt-like material (less than 43 microns) accounts for only 5.9 percent of the total solids, but it accounts for about 25 percent of the oxygen demand and from 30 to 50 percent of the algal nutrients. This concentration of pollutants in the very fine material is important because the catchbasin does not efficiently trap particles in this size range and thus allows a large percentage of these pollutants to pass through.

TABLE 14. CONTAMINANT CHARACTERISTICS AND QUANTITY SUMMARY [66]

Measured constituents	Weighted mean for all samples, kg/curb km (lb/curb mi)
Total solids	395 (1,400)
Oxygen demand	
BOD_5	3.8 (13.5)
COD	27 (95)
Volatile solids	28 (100)
Algal nutrients	
Phosphates	0.3 (1.1)
Nitrates	0.026 (0.094)
Kjeldahl nitrogen	0.62 (2.2)
Bacteriological	
Total coliforms, org/curb mi[a]	99×10^9
Fecal coliforms, org/curb mi	9.6×10^9
Heavy metals	
Zinc	0.18 (0.65)
Copper	0.06 (0.20)
Lead	0.16 (0.57)
Nickel	0.01 (0.05)
Mercury	0.02 (0.073)
Chromium	0.03 (0.11)
Pesticides	
p, p-DDD	$19 (67) \times 10^{-6}$
p, p-DDT	$17 (61) \times 10^{-6}$
Dieldrin	$6.8 (24) \times 10^{-6}$
Polychlorinated biphenyls	$310 (1,100) \times 10^{-6}$

a. The term "org" refers to the number of coliform organisms observed.

TABLE 15. FRACTION OF POLLUTANT ASSOCIATED WITH EACH PARTICLE SIZE RANGE, PERCENT BY WEIGHT [66]

Constituent	Particle size, μ					
	>2,000	840-2,000	246-840	104-246	43-104	<43
Total solids	24.4	7.6	24.6	27.8	9.7	5.9
Volatile solids	11.0	17.4	12.0	16.1	17.9	25.6
BOD_5	7.4	20.1	15.7	15.2	17.3	24.3
COD	2.4	4.5	13.0	12.4	45.0	22.7
Kjeldahl nitrogen	9.9	11.6	20.0	20.2	19.6	18.7
Nitrates	8.6	6.5	7.9	16.7	28.4	31.9
Phosphates	0	0.9	6.9	6.4	29.6	56.2
Total heavy metals	16.3	17.5	14.9	23.5	----27.8----	
Total pesticides	0	16.0	26.5	25.8	----31.7----	

Catchbasin Loading Intensity

The principal factors affecting the loading intensity at any given site include the following: surrounding land use, the elapsed time since streets were last cleaned (either intentionally or by rainfall), local traffic volume and character, street surface type and condition, public works practices, and season of the year [66].

In addition to the street surface contaminants, other materials, such as crankcase drainings, leaves, and grass clippings, are frequently discarded into catchbasins. This additional loading is highly variable, highly polluting, and difficult to estimate. A survey of San Francisco catchbasins, which illustrates the wide range of pollutant loading, is shown in Table 16.

Sediment Pollution

Although the sedimentation problem is primarily related to the runoff that enters streams directly rather than the runoff that flows through the storm drainage system, it is obvious that self-cleaning storm drains could contribute large quantities of sediment to waterways. These sediments can damage biological structures, bury organisms, and clog respiratory, feeding, and digestive organs [66]. In addition, sediment can contribute to flooding problems by raising stream beds and clogging drainage structures. Increased water treatment costs are associated with increased turbidity of the water. Decreased reservoir capacity caused by sedimentation is an expense that can be quite large.

TABLE 16. ANALYSIS OF CATCHBASIN CONTENTS, CITY OF SAN FRANCISCO, 1970 [65]

Catchbasin location	First sampling series, mg/L				Second sampling series, mg/L			
	COD	BOD_5	Total N	Total P	COD	BOD_5	Total N	Total P
Plymouth and Sadowa	3,860	190	10.9	<0.2	8,610	122	2.8	0.3
7th and Hooper	15,000	430	33.2	<0.2	2,570	170	2.0	<0.2
Yosemite	739	11	1.8	<0.2	21,400	120	4.6	<0.2
40th and Moraga	9,060	40	16.1	<0.2	51,000	130	12.0	<0.2
Mason and O'Farrell	8,100	130	29.7	<0.2	7,720	85	16.5	<0.2
32nd and Taraval	153	5	0.5	<0.2	708	15	1.4	<0.2
Haight and Ashbury	37,700	1,500	1.4	<0.2	143,000	420	14.6	<0.2
Marina area	701	100	7.0	<0.2	8,600	40	0.5	<0.2
Montgomery Street	6,440	390	18.8	<0.2	8,160	300	3.9	<0.2
Webster and Turk	1,440	44	14.0	<0.2	....	...	....	...
Lower Selby	288	6	1.4	<0.2	....	...	....	...
Upper Mission	5,590	50	12.0	0.2	....	...	....	...

Note: Both sampling series were conducted in winter 1970. All values based on an analysis of total basin contents after complete mixing.

Increased sediment pollution is associated with construction and urbanization; the pollution usually decreases after the construction phase is completed. Predevelopment background sediment yields generally range from 7.0×10^4 to 17.5×10^4 kg/km^2·yr (200 to 500 tons/mi^2·yr) [105]. Sediment yields for various locations and conditions of land use are shown in Table 17.

SOLIDS WASHOFF

Solids movement phenomena from the surface of the street to the gutter, and then along the gutter to the inlet and into a catchbasin, are mainly a function of the following factors: rainfall intensity, longitudinal slope of street, cross slope of street, antecedent dry period, land use, size and shape of drainage area, type and condition of street surface, season of year, street sweeping program, size distribution and availability of solids, and possibly others.

TABLE 17. REPRESENTATIVE DATA ON SEDIMENT YIELD [105]

Location	Drainage area, km^2 (mi^2)	Sediment yield, $kg/km^2 \cdot yr$ ($tons/mi^2 \cdot yr$)	Condition
Johns Hopkins University, Baltimore, Md.	0.0065 (0.0025)	48.9×10^6 (140,000)	Construction site
Tributary Mineback Run, Towson, Md.	0.081 (0.031)	27.9×10^6 (80,000)	Commercial
Tributary, Kensington, Md	0.24 (0.091)	8.38×10^6 (24,000)	Housing subdivision
Oregon Branch, Cockeysville, Md.	0.61 (0.236)	25.1×10^6 (72,000)	Industrial park

On the basis of experimental studies, it has been concluded that:

1. The soluble fractions go into solution. The impacting raindrops and the horizontal sheetflow provide good mixing turbulence and a continuously replenished clean "solvent."

2. Particulate matter (from sand size to colloidal size) is dislodged from its resting place by the impact of falling drops. Once dislodged, even reasonably heavy particles will be maintained in a state of pseudo-suspension by the repeated impact of adjacent drops, creating a reasonably high general level of turbulence [66].

Various equations have been developed to represent the solids washoff phenomenon. Perhaps the most utilized is that developed for the Storm Water Management Model [81].

> At the start of the rain, the amount of a particular pollutant on surfaces which produce runoff (both impervious and pervious) will be P_o, pounds per subarea. Assuming that the pounds of pollutant washed off in any time interval, dt, are proportional to the pounds remaining on the ground, P, the first order differential equation is:
>
> $$\frac{-dP}{dt} = kP \qquad (3)$$
>
> which integrates to
>
> $$P_o - P = P_o(1-e^{-kt}) \qquad (4)$$
>
> in which $P_o - P$ equals the pounds washed away in the time, t.

In order to determine k, it was assumed that k would vary in direct proportion to the rate of runoff, r, or $k = br$. To determine b it was assumed that a uniform runoff of 0.5 inch per hour would wash away 90 percent of the pollutant in one hour. This leads to the equation:

$$P_o - P = P_o(1-e^{-4.6rt}) \qquad (5)$$

where r = Runoff rate (in./hr)
t = Time interval (hr)

The use of Equation 5 is illustrated in Section 7. Modifications to this equation by the University of Cincinnati [64] and URS Research Company [109] provide for use of alternate units and site specific data. In the Storm Water Management Model version, an availability factor "A" of pollutants available for washoff is used for site specific calibration.

SECTION 6

HYDRAULIC MODELING ANALYSES

In the preceding sections, the functions of catchbasins and design and maintenance practices were identified, and the principal variables believed to affect performance were reviewed with respect to the removal of pollutants found in stormwater. Through these studies it was observed that virtually no basic documentation exists on the operational characteristics of catchbasins. Specifically, no data were found relating performance to basin geometry, flow, influent solids gradation, and accumulated sediment within the basins. To fill this data gap, controlled hydraulic modeling analyses were performed and the results are presented in this section.

The following presentation is extracted and adapted from Hydro-Research-Science Project Report No. HRS-039-75 "Catchbasin Hydraulic Model Studies of Flow Conveyance and Pollution Control" by Dr. Alexander B. Rudavsky, November 1975, performed under subcontract to this study.

OBJECTIVES

The flow-through pattern in catchbasins involves a three-dimensional flow, the configuration and complexity of which depend on the shape of the structure and the peripheral flow conditions. Such flows are complex and not subject to computational analysis. To analyze the flow patterns in existing catchbasins and to develop a design for future units, modeling techniques are imperative. Also, an experimental approach through model studies is required to assess the efficiency of solids capture quantitatively.

The objectives of the adopted modeling program were to test and document the following:

- Flow-through variations from 5.7 to 175.6 L/s (0.2 to 6.2 cfs), approximately 4 to 100 percent of maximum expected basin inflows

- Basin geometry variations in barrel diameter, outlet pipe diameter, barrel height, and barrel storage height (defined as height of outlet pipe invert above base)

- Outlet discharge controls, both open and trapped, for conditions from free flow to complete submergence

- Sediment capture as a function of gradation and accumulated sediment

- Performance associated with a recommended design configuration

EXPERIMENTAL SETUP

The setup for the catchbasin experimental program, as shown in Figure 8, consisted of three main components: (1) the catchbasin model, (2) the peripheral simulation of inlet and outlet conditions, and (3) the auxiliary appurtenances, including supportive machinery and storage basins. Model to prototype dimensions were fixed at undistorted linear scale ratios of 1:2.72 or 1:3.40, depending on the prototype barrel diameter simulated.

Components

The catchbasin model consisted of a multisectioned barrel with a movable bottom and two interchangeable outlet pipes, as shown in Figure 9. Bolted and pressure-tight connections provided the flexibility of substituting and removing sections to meet the full range of geometric configurations required. Each component was constructed of transparent plastic, permitting direct observation of the flow when illuminated.

The peripheral flow conditions were simulated by a partial representation of the street, the inlet opening with a grating, and the outlet pipe section, as shown in Figure 10. The street inflow conditions were simulated simply by inclining the surface platform 10 percent longitudinally and 20 percent transversely. The square grating was movable so that the bars could run parallel to, or across, the gutter flow. The outlet pipe was set at an angle of 5.4° below horizontal to force a critical control section at its entry.

Auxiliary equipment included (1) upstream and downstream tanks, (2) a sump to store water, (3) a centrifugal circulating water pump, (4) a system of discharge valves and butterfly regulating valves, (5) a solids feed system and a trap basin to avoid recirculating solids with the water, and (6) a metering system for measuring elevations, velocities, and discharges. In the sediment capture portions of the testing, commercial grade sands and ground sands, as well as a synthesized graded sand mixture, were used.

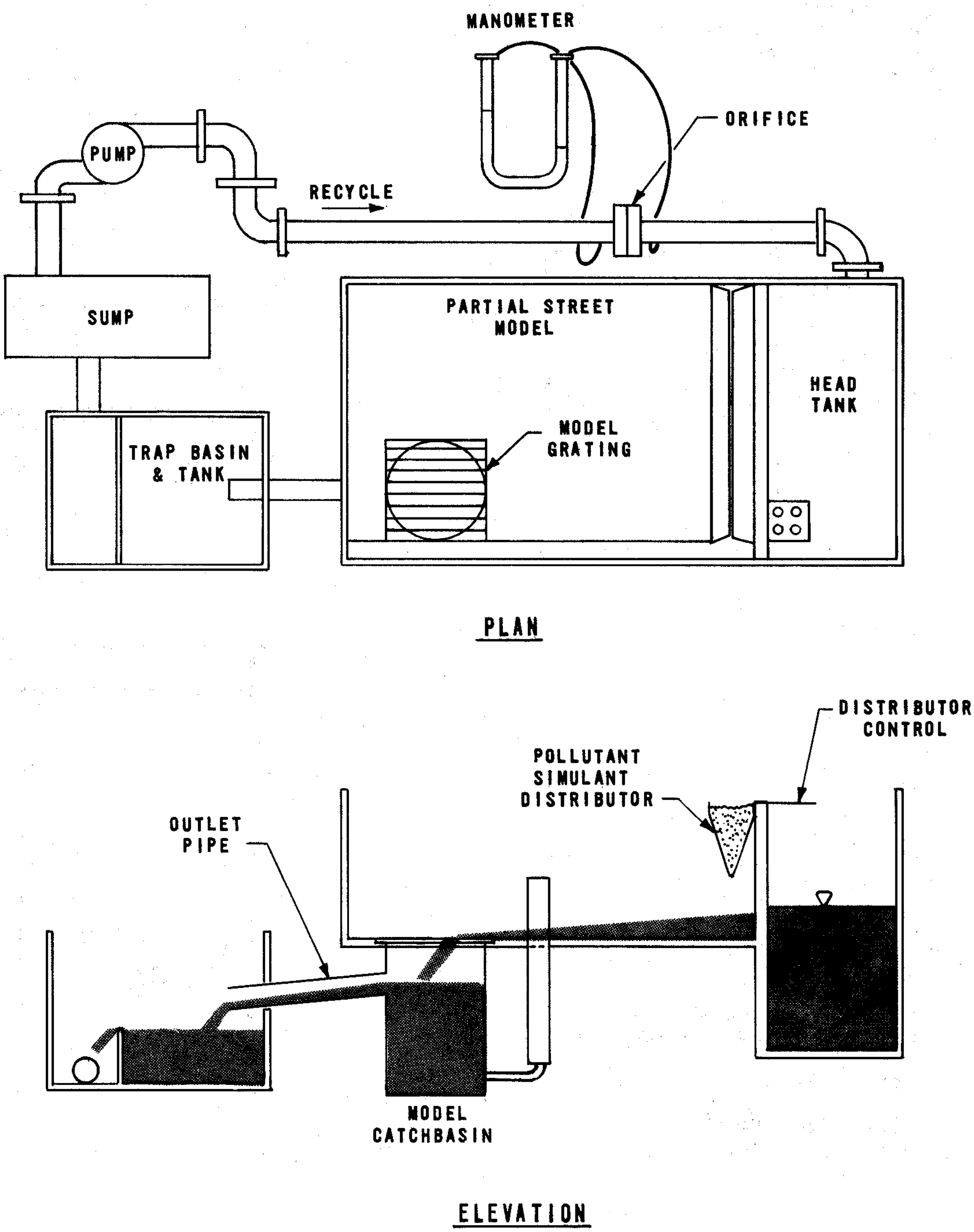

Figure 8. Experimental setup.

NOTE: DIMENSIONS SHOWN ARE IN FEET CONVERTED TO PROTOTYPE SCALE (SCALE 1:2.72). TO CONVERT TO cm MULTIPLY BY 30.48.

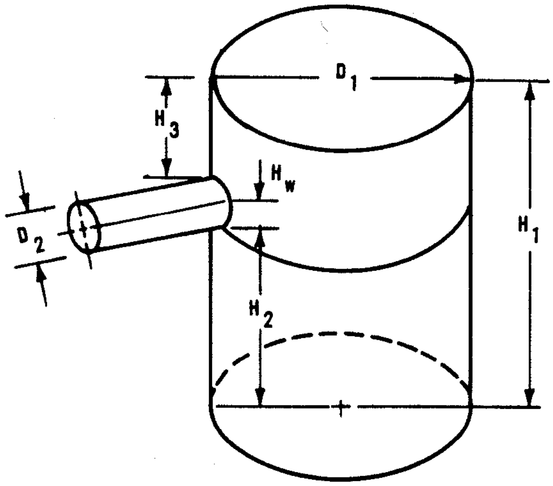

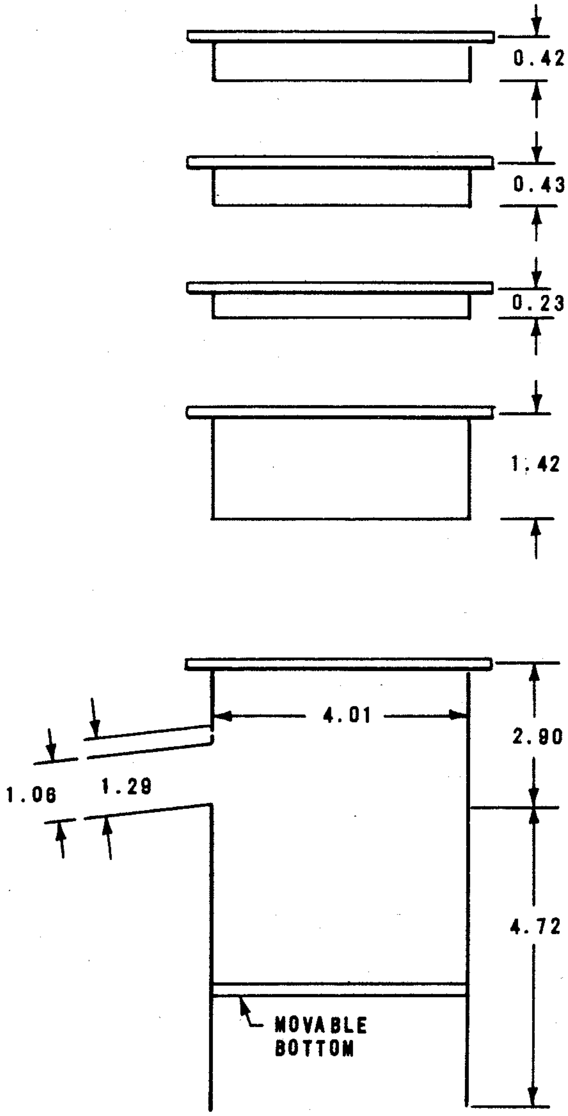

LEGEND

H_1	BARREL HEIGHT
H_2	BARREL STORAGE HEIGHT
H_3	HEIGHT FROM SOFFIT OF OUTLET PIPE TO TOP OF INLET GRATING
H_w	DISCHARGE HEAD (HEADWATER) ABOVE INVERT UNDER DISCHARGE Q
D_1	BARREL DIAMETER
D_2	OUTLET PIPE DIAMETER

Figure 9. Model catchbasin.

Photograph 1

Upstream view of partial street model with the view of head basin and the opening for grating insert.

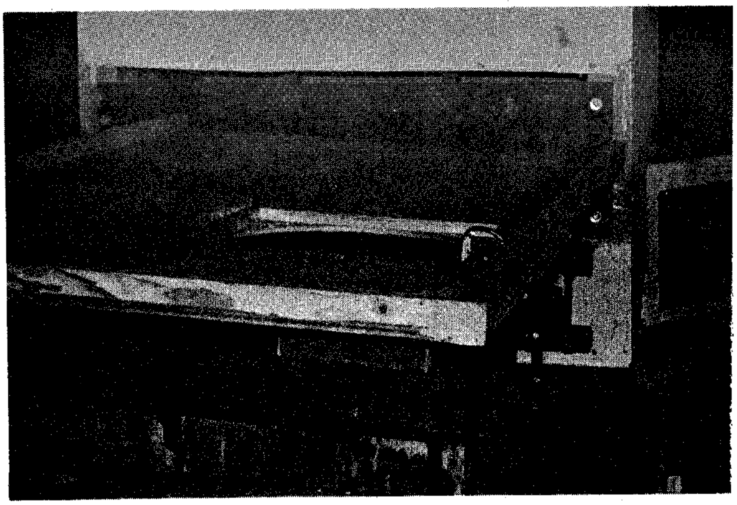

Photograph 2

Close-up view of model grating.

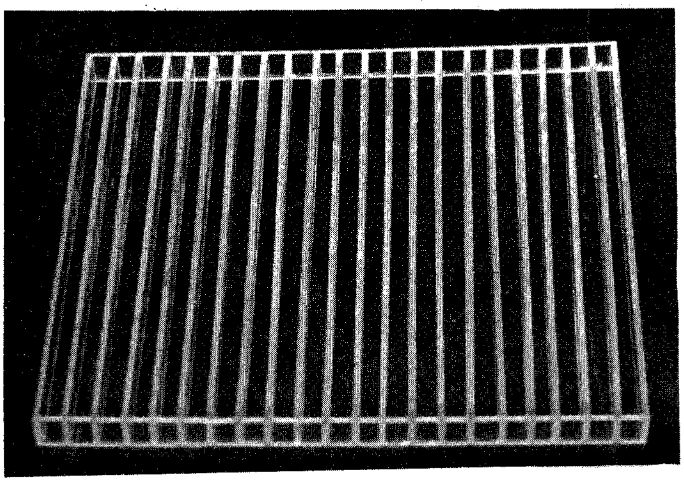

Photograph 3

Overall view of catchbasin barrel assembled.

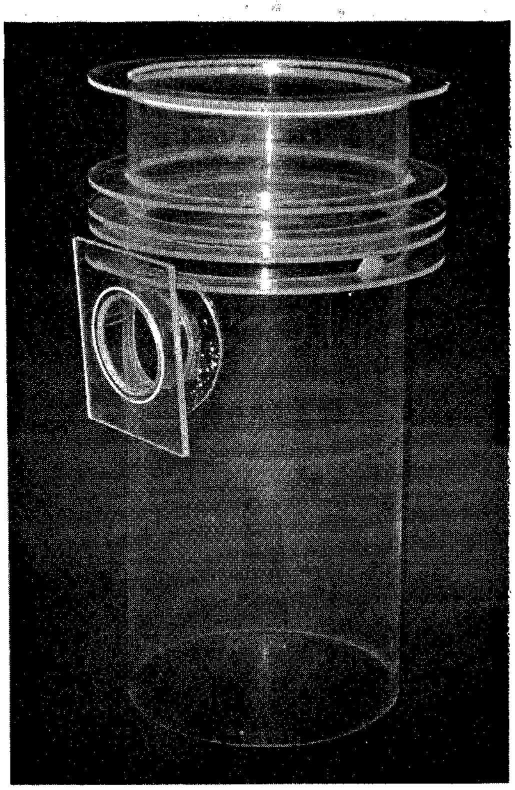

Figure 10. Model components prior to assembly.

Model Laws and Dimensional Analysis

The mathematical relationships between the model and the prototype, based on the Froude law, are summarized in Table 18. These scale relationships were used to transfer quantitatively the discharge, depth of flow, and velocities from the model to the prototype. Unless otherwise designated or self-evident, only prototype equivalents are presented.

TABLE 18. MODEL TO PROTOTYPE RELATIONSHIPS

Dimension	Ratio of model to prototype	Scale relationships	
Length	$L_r = \frac{L_m}{L_p}$	1:2.72	1:3.40
Area	$A_r = (L_r)^2$	1:7.40	1:11.56
Time	$T_r = (L_r)^{1/2}$	1:1.65	1:1.84
Velocity	$V_r = (L_r)^{1/2}$	1:1.65	1:1.84
Discharge	$Q_r = (L_r)^{5/2}$	1:12.20	1:31.32
Roughness	$n_r = (L_r)^{1/6}$	1:1.18	1:1.23

Note: m = model; p = prototype; r = ratio of model to prototype

Since complete dynamic similarity and accurate reproduction of some prototype properties are not possible, some limitations must be imposed on the model results:

- Measurements of discharge elevations and velocity can be transferred without reservation.
- Since it is not feasible to reproduce the roughness of a concrete surface in a plexiglass model of this scale, some differences in conveyance efficiencies can result. In this case, the differences are considered negligible.
- Air entrainment cannot be modeled by the Froude law alone, and there is now no acceptable method of correlating air entrainment between the model and prototype.
- Grain size dimensioning is based on settlement velocities and subject to many practical limitations. Thus, capture efficiencies are presented as a design guide and not as precise research data.

Dimensional analysis techniques were used to identify and group the significant variables.

EXECUTION

The hydraulic modeling was carried out in four phases:

- Phase 1. An experimental analysis of flow conditions in catchbasins representing current practice
- Phase 2. A selective repetition of Phase 1 tests with standard inlet and outlet modifications
- Phase 3. A series of runs to evaluate sediment capture
- Phase 4. The development and verification of flow conditions in the recommended catchbasin design

Prototype equivalents of variables used in the experimentation are listed in Table 19. Complete tests were run in four physical groupings (based on the ratio of barrel diameter to outlet diameter), three barrel heights (long, medium, and short), and two storage depths (deep and shallow), for a total of 24 discrete configurations.

TABLE 19. PRINCIPAL VARIABLES TESTED

Variable	Range
Discharge, L/s (cfs)	Q_{max} = 178.4 (6.3) Q_{des} = 35.4 (1.25) also Q_{small} = 14.2 (0.5) Q_{min} = 7.1 (0.25)
Barrel diameter, cm (ft)	$(D_1)_{max}$ = 152.4 (5.0) $(D_1)_{min}$ = 121.9 (4.0)
Barrel height, cm (ft)	$(H_1)_{max}$ = 243.8 (8.0) $(H_1)_{medium}$ = 182.9 (6.0) $(H_1)_{min}$ = 121.9 (4.0)
Barrel storage height, cm (ft)	$(H_2)_{max}$ = 121.9 (4.0) (50% of $H_{1\ max}$) $(H_2)_{max}$ = 30.5 (1.0) (25% of $H_{1\ min}$)
Exit pipe diameter, cm (ft)	$(D_2)_{max}$ = 38.1 (1.25) $(D_2)_{max}$ = 30.5 (1.0)

Typically, the test procedure was as follows:

1. Set up components in selected configuration.
2. Apply maximum flow and observe approach conditions, flow over grating, and flow conditions in the basin and outlet.
3. Record headwater height (above the invert D_2) and flow patterns, including extensive photography.

4. Trim to next lower flow and repeat until all desired flows are covered.

5. Drain, change to next configuration, and repeat full sequence.

In Phase 3, where solids were applied, only a minimum of experimental setups were used because of the added long drying and weight checking periods required. The range of materials used was chosen from commercially available sand mixtures, defined by their commercial designations as No. 20, No. 30, No. 2, No. 57, and No. 84. Their respective sieve analyses are shown in Figure 11 along with the prototype gradation used by Sartor and Boyd [66].

A limited supportive program was executed to establish the significance of discharge, pollutant load concentration, and test duration to sediment capture results. Commercial No. 20 and No. 30 sands were discharged with different concentrations through a wide range of test durations. For example, No. 20 sand was run separately at a constant feed rate for 25.5, 10.3, and 5.8 minutes for a single discharge. In all of these studies, the retention characteristics appeared to be independent of the concentration, and the deposition was directly proportional to the length of run. Similar results were obtained using No. 2 sand, and it was concluded that the test durations could be uniformly fixed at a nominal 5 minutes for the Phase 3 and Phase 4 studies.

Note that in a typical 5-minute test under maximum flow conditions, over 53,000 L (14,000 gal.) of water was circulated through the test unit carrying approximately 7,100 g (16 lb) of simulant for a mean concentration of 133 mg/L. This is within the typical range expected in surface runoff from streets.

RESULTS

In expressing the experimental results, somewhat detailed descriptions are given for what may appear to the reader to be rather obvious conclusions. The intent is to maximize the benefits of this experimentation for potential future investigations as well as to satisfy the immediate study objectives.

Phase 1 - Hydraulics

In Phase 1, all 24 configurations were tested, and a discharge rating curve was constructed for each configuration. A preliminary assessment was made as to which basins were satisfactory, unsatisfactory, or marginal for sediment capture on the basis of observed turbulence and flow patterns.

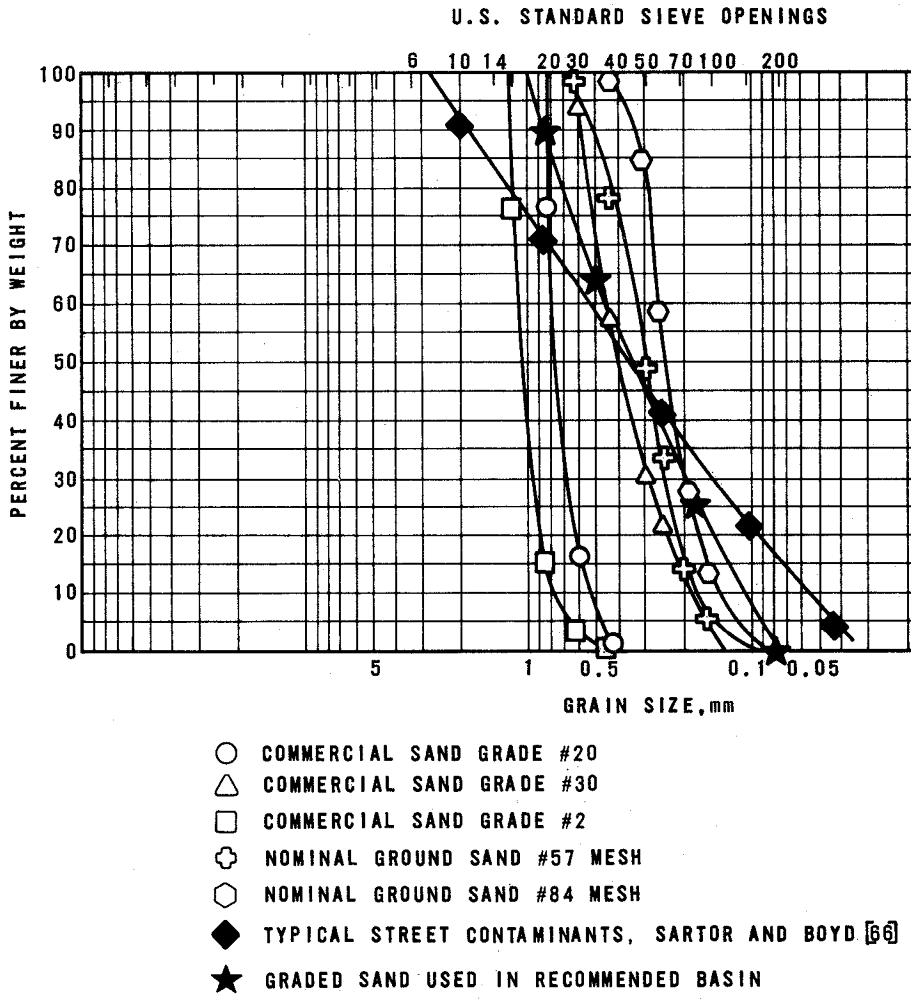

Figure 11. Sieve analyses of test simulants.

Two flow pattern groupings were evident: those influenced by the exit conditions and those generated in the storage basin.

Exit Conditions --

As shown in Figure 12, the outlet pipe controlled the flow through the following ranges, presented in the order of increasing flow: (1) open channel flow, controlled through weir control and directly related to critical depth at the outlet; (2) orifice control flow, controlled by the sharp edges of the entrance to the outlet pipe with subsequent open channel flow in the pipe itself; (3) short tube control flow, controlled in the outlet pipe with a short tube type of control of various lengths; and (4) pipe control with pressure flow existing in the outlet pipe and flowing completely full. Slug flow was also observed where the flow in the pipe contained large bubbles and represented unsteady flow conditions. With the exit pipe set very close to the grating at high discharges, the catchbasin filled up, overflowed, and became totally submerged.

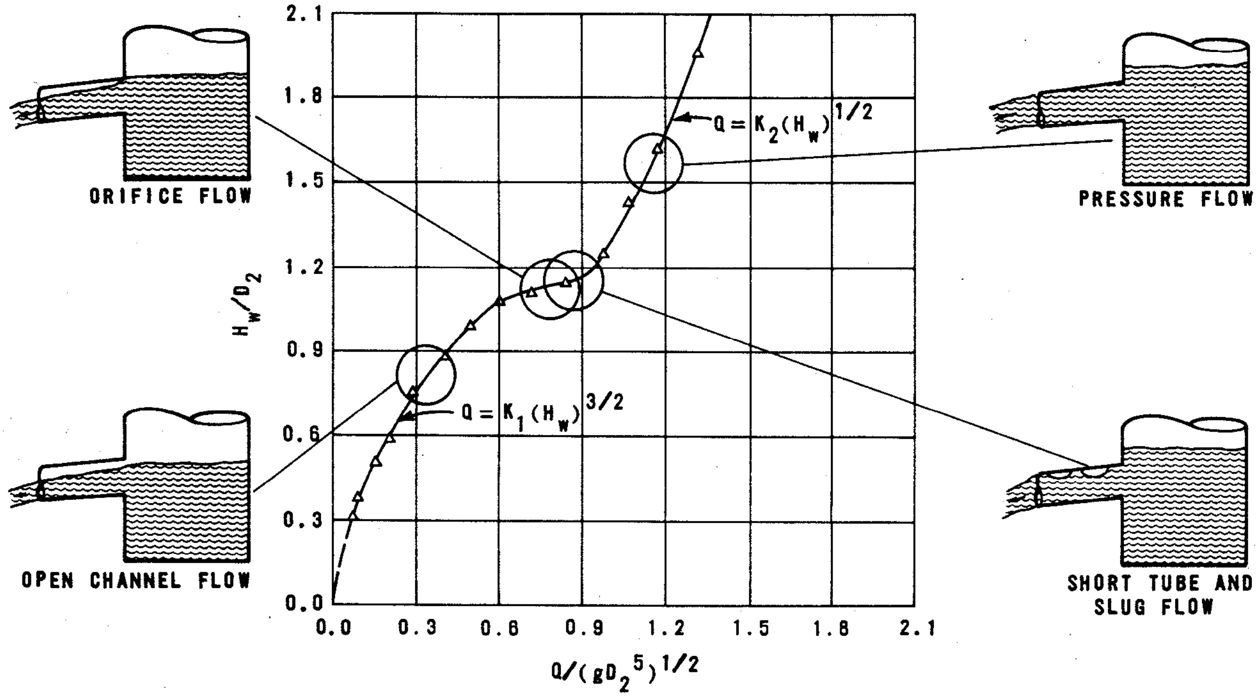

Figure 12. Typical discharge rating curve.

As shown in Figure 12, the discharge-to-headwater relationship can be directly associated to these flow conditions. For open channel flow with critical depth control, the relationship of discharge to headwater has an exponent of 3/2, indicating a large discharge capacity. The discharge-to-headwater relationship for pressure flow has an exponent of only 1/2, indicating a very small discharge capacity. Although the discharge rating curve for each catchbasin configuration is unique, all have the same characteristic shape.

Storage Basin--

Flow patterns in the storage basin depend on its volume, depth, and rate of discharge. The primary patterns are the jet descending from the grating and an eddy pattern induced by that jet in the storage basin. Distinct flow patterns were observed in the experimental program, ranging from a plunging jet for very large discharges inducing a macro eddy to a very weak descending jet sequence being dissipated in the basin. When the storage basin is shallow, the descending jet impinges upon the floor and can go both toward and away from the outlet.

The observed flow and control conditions are identified in Figure 13. Since both the exit conditions and storage basin flow patterns are unique to each basin configuration, the latter can be classified, on the basis of experimental observation, into three basic types: satisfactory, marginal, and unsatisfactory. Typical flow conditions in each broad classification are shown in Figure 14.

Summary--

A review of flow patterns controlled by exit conditions indicates that all flows less than 50 percent of maximum were open channel flows. This clearly indicates such a flow would be expected for the majority of flow patterns. Of the 24 basins investigated and summarized in Table 20, 8 showed satisfactory storage flow conditions (i.e., conditions conducive to solids capture), 4 were marginal, and 12 appeared unsatisfactory. Photographic documentation is presented in Figures 15 through 18.

Nominal catchbasin depths of 183 to 244 cm (6 to 8 ft) with 50 percent or greater storage depths ($H_2/D_2 \geq 2.4$) exhibit the best flow conditions for solids capture. The shallow storage configurations ($H_2/D_2 \geq 1.5$) invariably appeared unsatisfactory.

Phase 2 - Standard Modifications

In Phase 2 of the experimental program, the influence of standard modifications to catchbasin inlet and outlet controls was investigated. The first modification involved placing a hood over the entrance to the outlet pipe, and the second involved the addition of a curb protrusion above a portion of the grated inlet. Four catchbasin configurations were tested, all chosen from the marginal or unacceptable categories to magnify any improvements in flow patterns.

In Configuration 11 (Table 20) a small diameter, short height, but deep storage basin was tested first. The curb was moved out 15.2 cm (6 in.) into the gutter but was notched to fully expose the inlet grating, thus simulating a combination grating and curb inlet. The effect on the discharge rating curve was minimal, even under very unstable conditions. Testing the same basin without a protruding curb, but with a hood over the outlet to typify common gas traps, produced a radical change in discharge capacity and a substantially different rating curve. The dramatic decrease in discharge capacity can be observed in Figure 19. Investigation of the influence of the curb and hooded outlet in combination again showed the dominance of the hood's influence and the slight influence of the curb.

The tests were repeated for Configurations 23, 4, and 2 with similar results. From Phase 2 it was concluded that hooded entrances drastically changed the discharge rating curve,

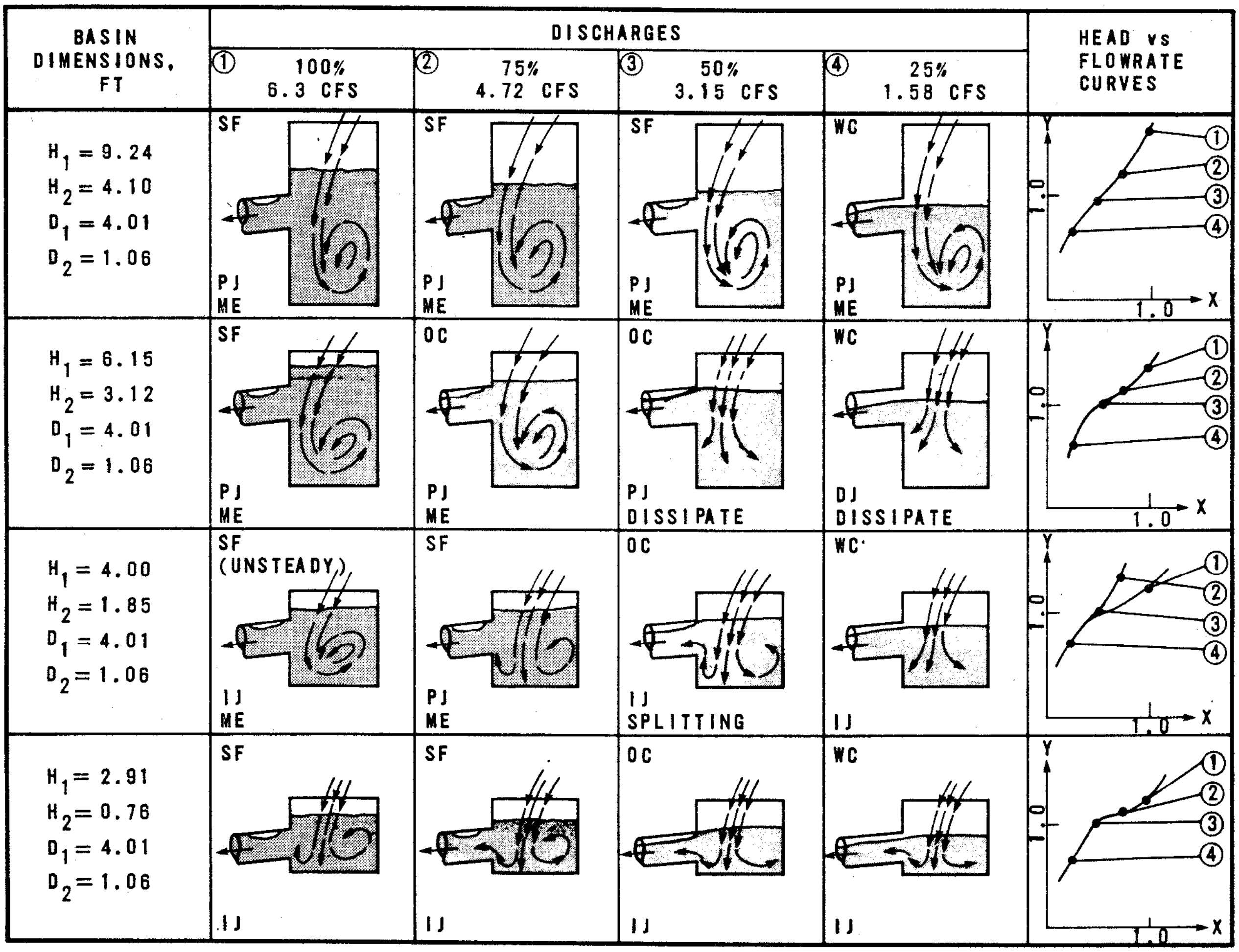

LEGEND

- H_1 TOTAL HEIGHT FROM BOTTOM TO TOP OF GRATING
- H_2 STORAGE BASIN HEIGHT
- D_1 BARREL DIAMETER
- D_2 EXIT PIPE DIAMETER
- X $Q/(gD_2^{\,5})^{1/2}$
- Y H_w/D_2

ABBREVIATIONS

- PJ PLUNGING JET
- IJ IMPINGING JET
- ME MACRO EDDIES
- OC ORIFICE CONTROL
- SF SLUG FLOW
- WC WEIR CONTROL
- DJ DISSIPATING JET

Figure 13. Observed flow conditions.

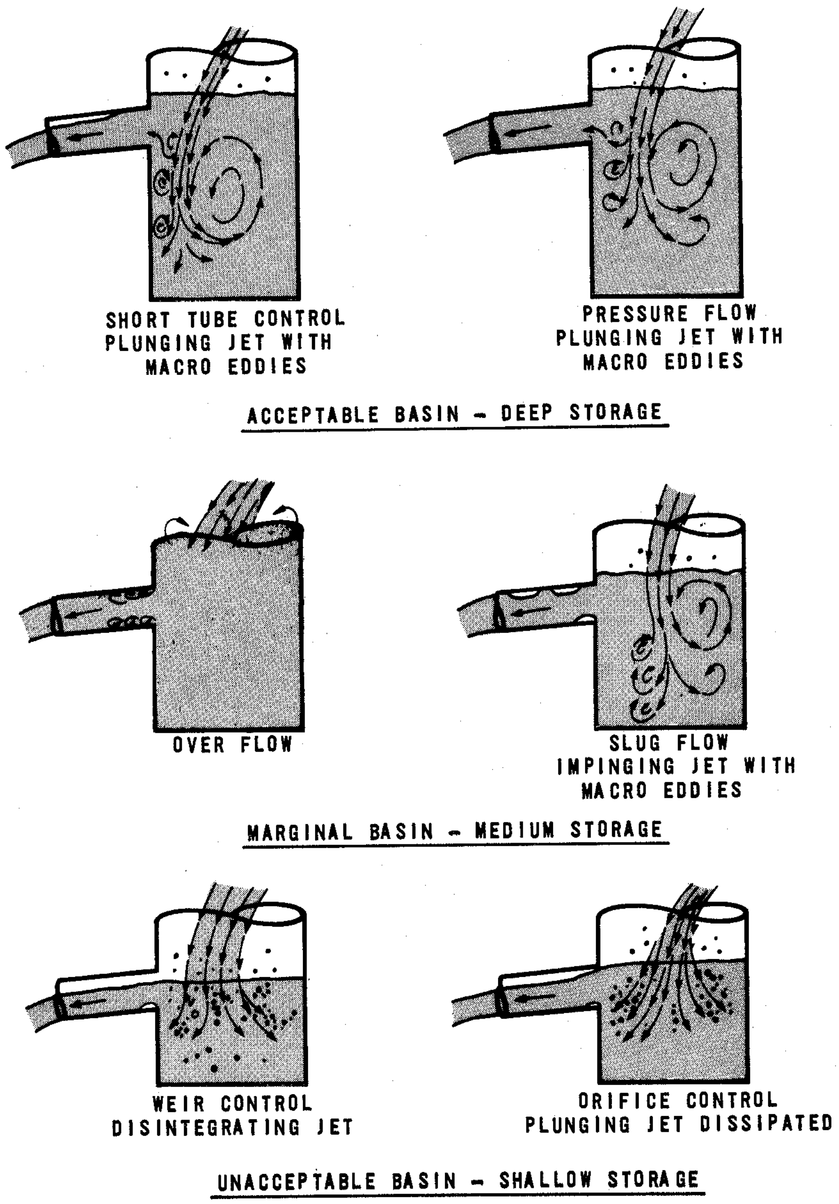

Figure 14. General performance classifications.

TABLE 20. SUMMARY OF PHASE 1 PROGRAM

Nominal physical parameters, ft[a]								Flow conditions, H_w/D_2								
								% discharge								
Barrel size	D_1	D_2	Barrel length	H_1	Storage	H_2	H_2/D_2	100	75	50	25	20	8	4	Remarks[b]	Basin configuration
Large	5.00	1.00	Long	8.00	Deep	4.00	4.00	1.22	1.11	0.93	0.64	0.57	0.32	....	S	1
				6.00	Shallow	1.50	1.50	1.22	1.13	0.91	0.64	0.55	....	....	U	2
			Medium	6.00	Deep	3.00	3.00	1.19	1.13	0.96	0.64	0.54	....	....	S	3
				4.50	Shallow	1.12	1.12	1.11	1.08	0.90	0.63	0.58	0.36	....	U	4
			Short	4.00	Deep	2.00	2.00	1.16	1.07	0.91	0.68	0.60	0.38	0.30	M	5
				3.00	Shallow	0.75	0.75	1.16	1.04	0.95	0.76	0.65	0.41	0.32	U	6
Small	4.00	1.00	Long	8.00	Deep	4.00	4.00	1.58	1.20	0.95	0.64	0.60	0.30	....	S	7
				6.00	Shallow	1.50	1.50	1.53	1.18	0.96	0.62	0.60	....	....	U	8
			Medium	6.00	Deep	3.00	3.00	1.22	1.10	1.00	0.68	0.60	....	....	S	9
				4.50	Shallow	1.12	1.12	1.40	1.12	0.96	0.64	0.58	....	....	U	10
			Short	4.00	Deep	2.00	2.00	1.25	1.35	0.98	0.70	0.62	....	....	M	11
				3.00	Shallow	0.75	0.75	1.24	1.11	1.03	0.67	0.60	0.40	0.32	U	12
Large	5.00	1.25	Long	8.00	Deep	4.00	3.20	1.32	1.10	1.00	0.68	0.60	....	....	S	13
				6.00	Shallow	1.50	1.20	1.03	0.93	0.70	0.49	0.42	....	....	U	14
			Medium	6.00	Deep	3.00	2.40	1.03	0.93	0.76	0.49	0.43	....	....	S	15
				4.50	Shallow	1.12	0.90	1.00	0.89	0.70	0.49	0.43	....	....	U	16
			Short	4.00	Deep	2.00	1.60	1.02	0.93	0.72	0.54	0.51	....	....	M	17
				3.00	Shallow	0.75	0.60	1.06	0.94	0.72	0.52	0.46	0.32	0.28		18
Small	4.00	1.25	Long	8.00	Deep	4.00	3.20	1.10	0.97	0.74	0.45	0.42	....	....	S	19
				6.00	Shallow	1.50	1.20	1.08	0.93	0.72	0.52	0.46	....	....	U	20
			Medium	6.00	Deep	3.00	2.40	1.08	0.89	0.68	0.52	0.47	....	....	S	21
				4.50	Shallow	1.12	0.90	1.14	1.00	0.77	0.52	0.46	0.28	....	U	22
			Short	4.00	Deep	2.00	1.60	1.08	0.90	0.78	0.53	0.46	....	....	M	23
				3.00	Shallow	0.75	0.60	1.11	0.98	0.75	0.51	0.46	0.29	0.23	U	24

a. 30.48 cm = 1 ft.

b. S = satisfactory storage; U = unsatisfactory storage; M = marginal storage.

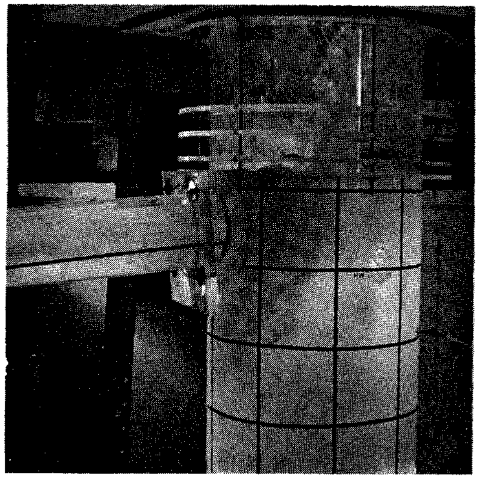

Photograph 4
Q = 5.43 cfs (86%) short tube control, plunging jet with macro eddy

$HW/D_2 = 1.12$ $Q/(gD_2^5)^{1/2} = 0.83$

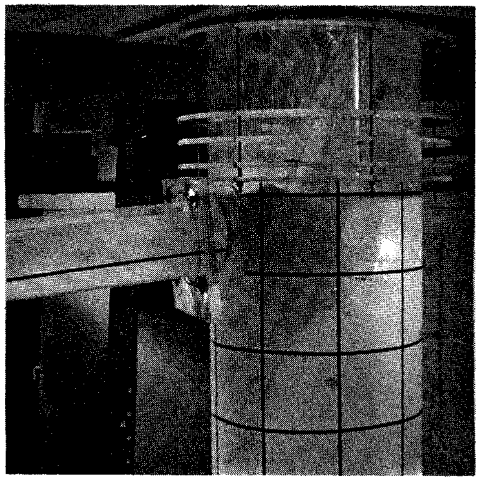

Photograph 5
Q = 4.06 cfs (64%) short tube control, plunging jet with macro eddy

$HW/D_2 = 1.02$ $Q/(gD_2^5)^{1/2} = 0.62$

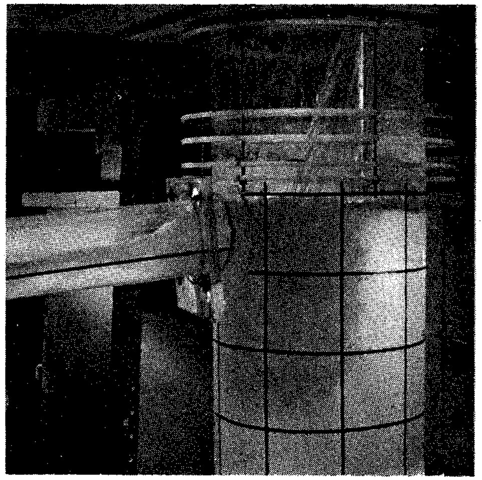

Photograph 6
Q = 2.72 cfs (43%) short tube almost orifice control, plunging jet with macro eddy

$HW/D_2 = 0.91$ $Q/(gD_2^5)^{1/2} = 0.42$

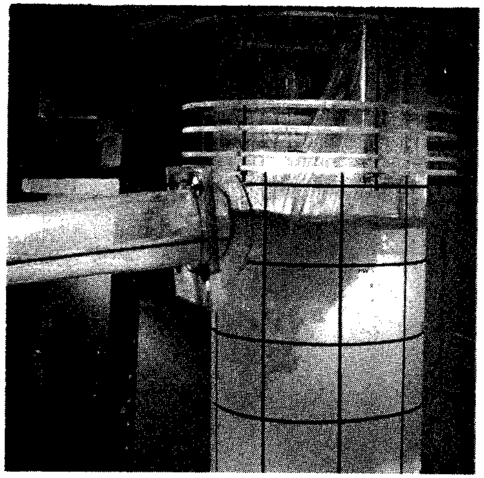

Photograph 7
Q = 1.36 cfs (22%) weir control, plunging jet with macro eddy

$HW/D_2 = 0.55$ $Q/(gD_2^5)^{1/2} = 0.21$

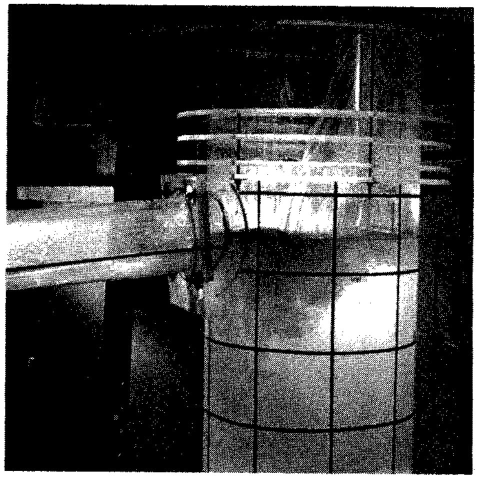

Photograph 8
Q = 1.08 cfs (17%) weir control, plunging jet with macro eddy

$HW/D_2 = 0.48$ $Q/(gD_2^5)^{1/2} = 0.16$

$D_1 = 4.01$ ft; $D_2 = 1.06$ ft

$H_1 = 9.24$ ft; $H_2 = 4.10$ ft

$H_3 = 3.85$ ft; $D_1/D_2 = 3.78$

$H_1/D_2 = 8.72$; $H_2/D_2 = 3.87$

$H_3/D_2 = 3.63$

Control and Flow Conditions
In Very Deep Catchbasin ($H_1 = 9.24$ ft)

Satisfactory Storage Basin

Figure 15. Photographic record - configuration 7.

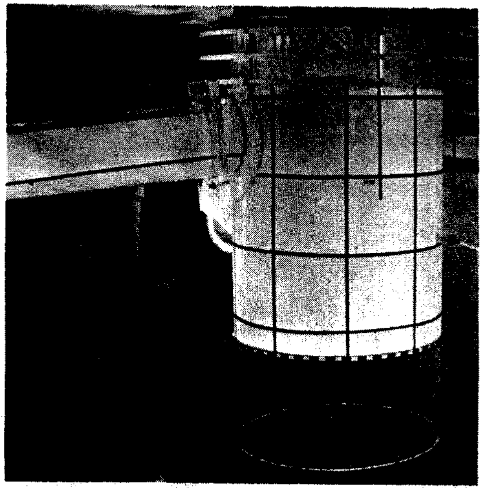

Photograph 9
Q = 5.43 cfs (86%) diving jet and macro eddies

$HW/D_2 = 1.17$ $Q/(gD_2^5)^{1/2} = 0.83$

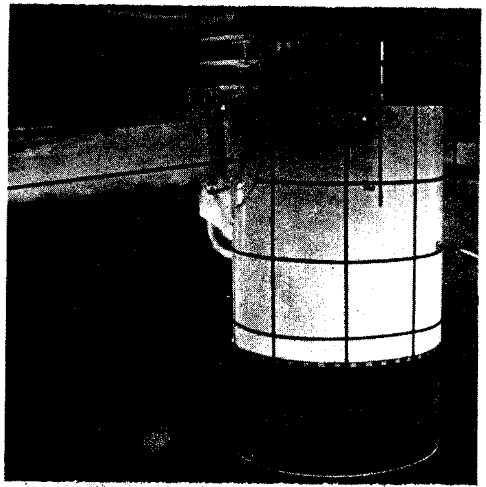

Photograph 10
Q = 4.06 cfs (64%) diving jet and macro eddies

$HW/D_2 = 1.06$ $Q/(gD_2^5)^{1/2} = 0.62$

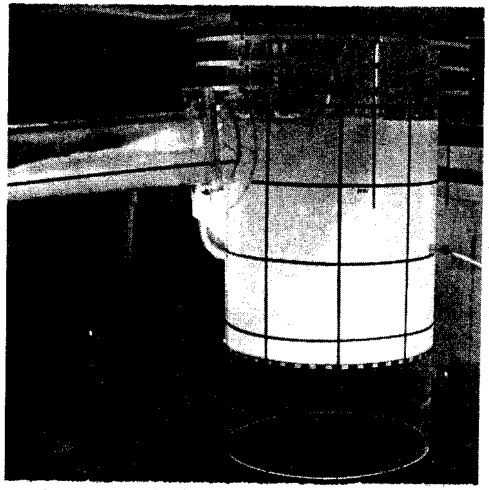

Photograph 11
Q = 2.72 cfs (43%) orifice control, diving jet dissipating

$HW/D_2 = 0.93$ $Q/(gD_2^5)^{1/2} = 0.42$

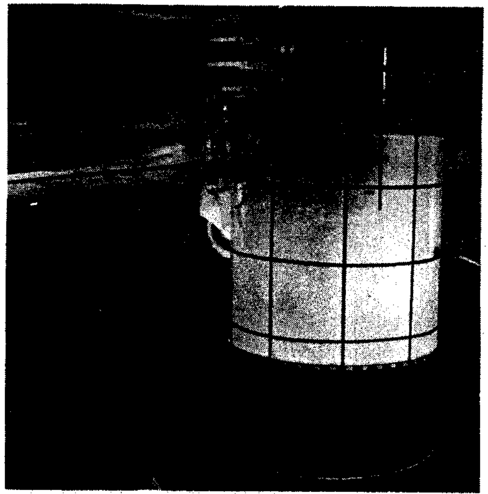

Photograph 12
Q = 1.36 cfs (22%) weir control, diving jet dissipating

$HW/D_2 = 0.60$ $Q/(gD_2^5)^{1/2} = 0.21$

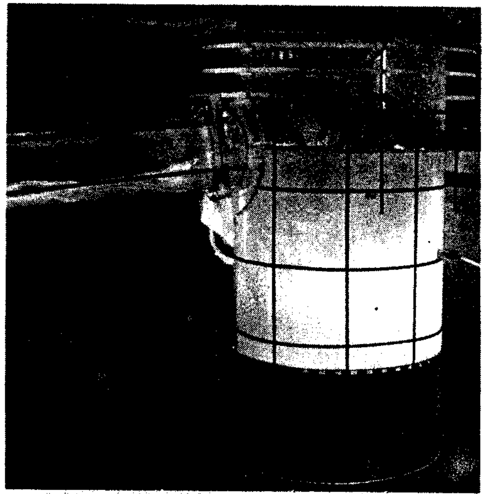

Photograph 13
Q = 1.08 cfs (17%) weir control, diving jet dissipating

$HW/D_2 = 0.54$ $Q/(gD_2^5)^{1/2} = 0.16$

$D_1 = 4.01$ ft; $D_2 = 1.06$ ft

$H_1 = 6.15$ ft; $H_2 = 3.12$ ft

$H_3 = 1.97$ ft; $D_1/D_2 = 3.78$

$H_1/D_2 = 5.80$; $H_2/D_2 = 2.94$

$H_3/D_2 = 1.86$

Control and Flow Conditions
In Deep Catchbasin ($H_1 = 6.15$ ft)

Satisfactory Storage Basins

Figure 16. Photographic record - configuration 9.

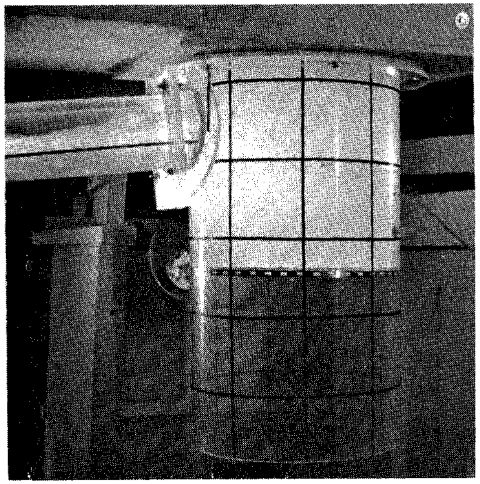

Photograph 14
Q = 5.43 cfs (86%) impinging jet
HW/D_2 = 1.17 to 1.67 $Q/(gD_2^5)^{1/2}$ = 0.83

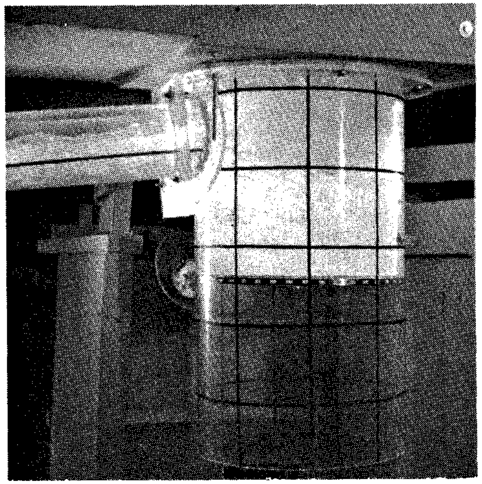

Photograph 15
Q = 4.06 cfs (64%) impinging jet
HW/D_2 = 1.18 $Q/(gD_2^5)^{1/2}$ = 0.62

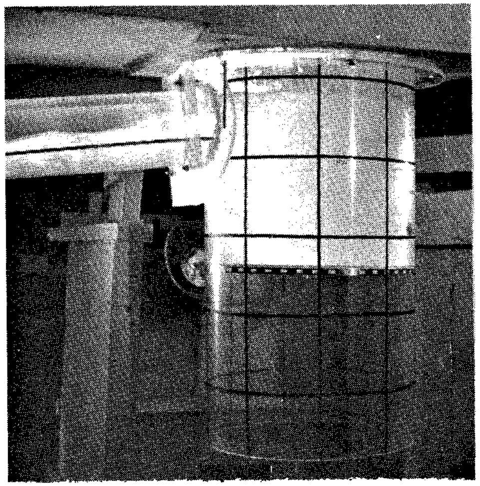

Photograph 16
Q = 2.72 cfs (43%) impinging jet
HW/D_2 = 0.94 $Q/(gD_2^5)^{1/2}$ = 0.42

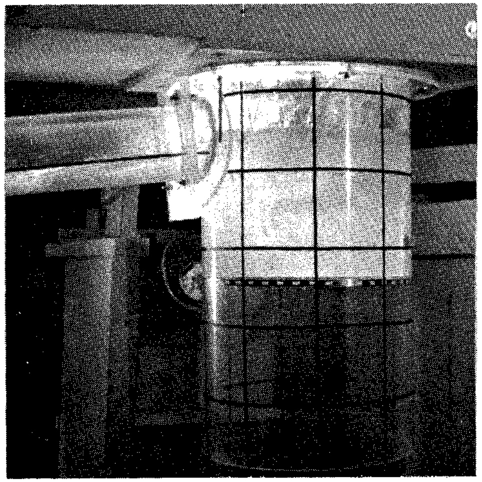

Photograph 17
Q = 1.36 cfs (22%) dissipating jet
HW/D_2 = 0.62 $Q/(gD_2^5)^{1/2}$ = 0.21

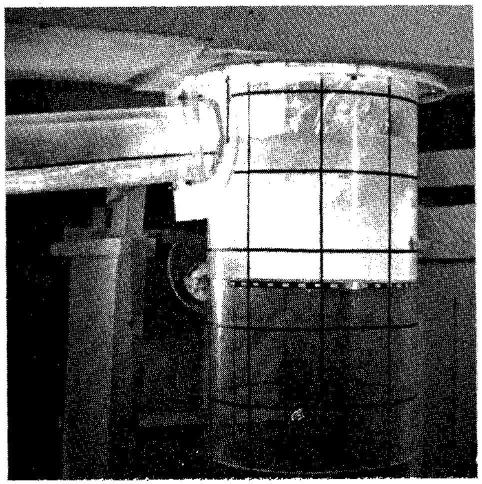

Photograph 18
Q = 1.08 cfs (17%) dissipating jet
HW/D_2 = 0.56 $Q/(gD_2^5)^{1/2}$ = 0.16

D_1 = 4.01 ft; D_2 = 1.06 ft

H_1 = 4.00 ft; H_2 = 1.85 ft

H_3 = 1.09 ft; D_1/D_2 = 3.78

H_1/D_2 = 3.77; H_2/D_2 = 1.74

H_3/D_2 = 1.03

Control and Flow Conditions
In a Medium deep Catchbasin (H_1 = 4.00 ft)

Marginal Storage Basin

Figure 17. Photographic record - configuration 11.

Photograph 19
Q = 5.43 cfs (86%) short tube control, impinging jet
$HW/D_2 = 1.05$ $Q/(gD_2^5)^{1/2} = 0.83$

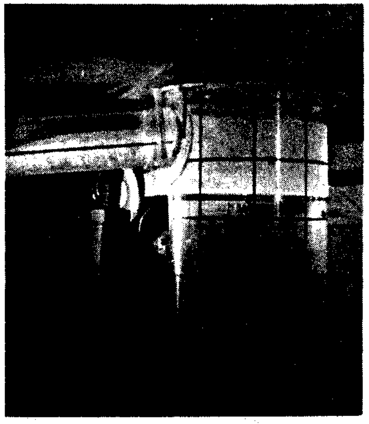

Photograph 20
Q = 4.06 cfs (64%) short tube control, impinging jet
$HW/D_2 = 1.08$ to 1.23 $Q/(gD_2^5)^{1/2} = 0.64$

Photograph 21
Q = 2.72 cfs (43%) weir control, impinging jet
$HW/D_2 = 0.87$ $Q/(gD_2^5)^{1/2} = 0.42$

Photograph 22
Q = 1.36 cfs (22%) weir control, impinging jet
$HW/D_2 = 0.69$ $Q/(gD_2^5)^{1/2} = 0.21$

Photograph 23
Q = 1.08 cfs (17%) weir control, impinging jet
$HW/D_2 = 0.59$ $Q/(gD_2^5)^{1/2} = 0.16$

Photograph 24
Q = 0.43 cfs (6.8%) weir control, impinging jet
$HW/D_2 = 0.34$ $Q/(gD_2^5)^{1/2} = 0.066$

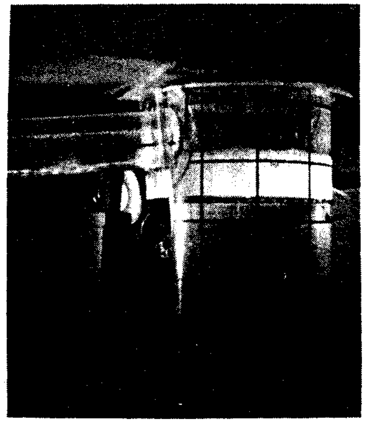

Photograph 25
Q = 0.22 cfs (3.4%) weir control, impinging jet
$HW/D_2 = 0.27$ $Q/(gD_2^5)^{1/2} = 0.034$

$D_1 = 5.01$ ft; $D_2 = 1.06$ ft

$H_1 = 3.65$ ft; $H_2 = 0.95$ ft

$H_3 = 1.64$ ft; $D_1/D_2 = 4.72$

$H_1/D_2 = 3.44$; $H_2/D_2 = 0.90$

$H_3/D_2 = 1.54$

Control and Flow Conditions
In Very Shallow Basin ($H_1 = 3.65$ ft)

Unsatisfactory Storage Basin

Figure 18. Photographic record - configuration 6.

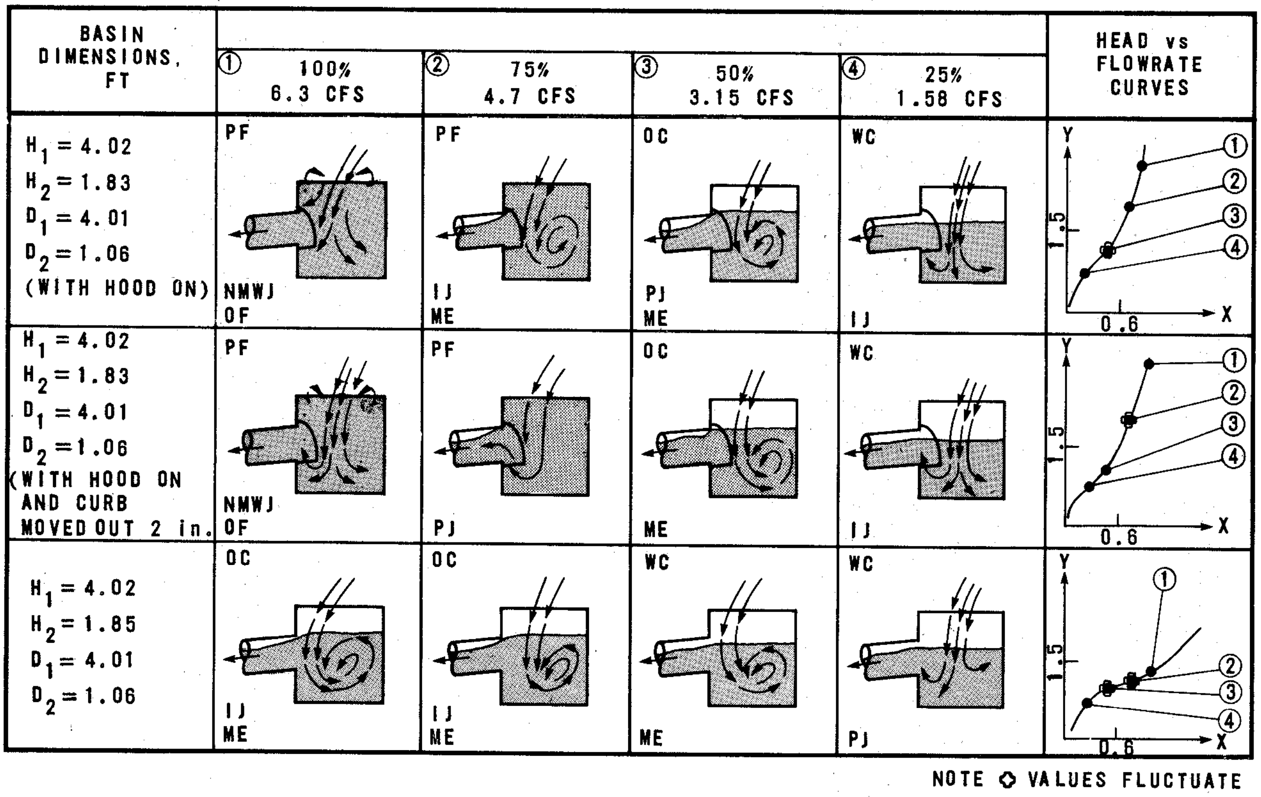

LEGEND

H_1	TOTAL HEIGHT FROM BOTTOM TO TOP OF GRATING
H_2	STORAGE BASIN HEIGHT
D_1	BARREL DIAMETER
D_2	EXIT PIPE DIAMETER
X	$Q/(gD_2^{\,5})^{1/2}$
Y	H_w/D_2

ABBREVIATIONS

PJ	PLUNGING JET
IJ	IMPINGING JET
ME	MACRO EDDIES
OC	ORIFICE CONTROL
SF	SLUG FLOW
WC	WEIR CONTROL
PF	PRESSURE CONTROL
OF	OVER FLOW
NMWJ	NO MAIN WATER JET

Figure 19. Influence of modifications on marginal basin.

especially in the range of orifice and short tube control, and drastically reduced the discharge capacity. Compared to flows under unhooded conditions, the influences of curb protrusions seemed to be minor.

Phase 3 - Sediment Capture

In Phase 3, qualitative evaluation procedures were used to define sediment retention for various conditions and these data were used to develop an optimal design configuration. Generally, the simulant approximated the medium-sized pollutant solids used in other experimental programs. Where justified, supplemental tests were run with finer or graded materials. Multiple flowrates were attempted, but emphasis was placed in the middle ranges.

Initial Configuration--

Configuration 16 (large diameter, medium height, shallow storage) was selected for the initial tests to set a base from which improvements could be expected. The simulant was commercial grade No. 30 sand. A maximum discharge of 232 L/s (8.2 cfs), 130 percent of expected maximum, plus simulant, was applied to a clean basin. This resulted in a solids capture on only 3.4 percent by dry weight (i.e., 96.6 percent of the simulant sluiced through the test unit and was recovered from the discharge sump).

The test was restarted using a flowrate of 152.9 L/s (5.4 cfs) and observation of the retention characteristics showed that 77 percent of the material sluiced through and only 23 percent was retained in the barrel. Short tube or orifice flow prevailed. Next, the discharge was further reduced to 76.5 L/s (2.7 cfs), resulting in open channel, weir control, and the retained material increased to 44 percent. Considering that the basic configuration was in the unsatisfactory range, the retention under the 76.5 L/s (2.7 cfs) flow was surprisingly good.

Seeking improvement, however, the storage basin depth was doubled ($H_2/D_2 = 1.74$, Configuration 17). The overall depth was increased from approximately 122 to 152 cm (4 to 5 ft), and the same 76.5 L/s (2.7 cfs) flowrate was applied. The retention jumped to 72 percent, indicating a marked advantage for deeper basins, particularly in the storage zone.

Deep Basins--

The deepest basin geometry, Configuration 1, was attempted next, holding the flowrate at 76.5 L/s (2.7 cfs). The retention showed a further improvement to 80 percent, which appears optimal for this flowrate. Then, the deepest 122 cm (4 ft) diameter basin, Configuration 7, was tested at a discharge of 152.9 L/s (5.4 cfs), and the retention was a satisfactory 42 percent, nearly twice the efficiency of the shallow basin used in the initial test.

Accumulation Impacts--

Using Configuration 1, a series of 10 consecutive runs were executed in which the solids were left to accumulate in the basin. Using No. 30 sand, the captured sediment increased rather uniformly, with 73 percent or better sediment retained in each run through the first five runs. At this point, corresponding to a volumetric level approaching 0.4 H2, the capture efficiency dropped off sharply and became erratic.

Fine Material--

Finer composition sands (specific gravity 2.65) were used in two cases and mesh 100 gilsonite (specific gravity 1.06) was used in one case. A mesh 250 material was also used. Gilsonite and mesh 250 material sluiced right through the system under a discharge of 76.5 L/s (2.7 cfs). The fine sands results are reported under Phase 4.

Phase 4 - Recommended Design

From the studies conducted herein and the information from the earlier sections, a simple recommended design evolved that is appropriate for either 122 or 152 cm (4 or 5 ft) diameter basins, as shown in Figure 20. The circular cross-section is preferred from a cleaning and prefabrication viewpoint. The dimension from the outlet pipe crown to the street or inlet grade is primarily a structural consideration, as it contributes little to the hydraulic performance. To be cost effective, the maximum depth should be incorporated in the storage zone H_2 and the outlet pipe D_2 should be sufficiently large to pass most flows under open channel conditions.

In Phase 4, a complete series of rating and evaluation tests were performed using the model in the recommended design configuration.

Hydraulic Performance--

The discharge rating curve for the recommended basin is plotted on a dimensionless basis in Figure 21 with the identified flow conditions. The corresponding photographic record is shown in Figure 22. The discharge rating curve fixed the relationship between discharge Q, discharge head above outlet pipe invert H_w, and outlet diameter D_2 assuming free discharge.

Open channel flow conditions are maintained in the outlet pipe for flows up to approximately 50 percent of the design maximum.

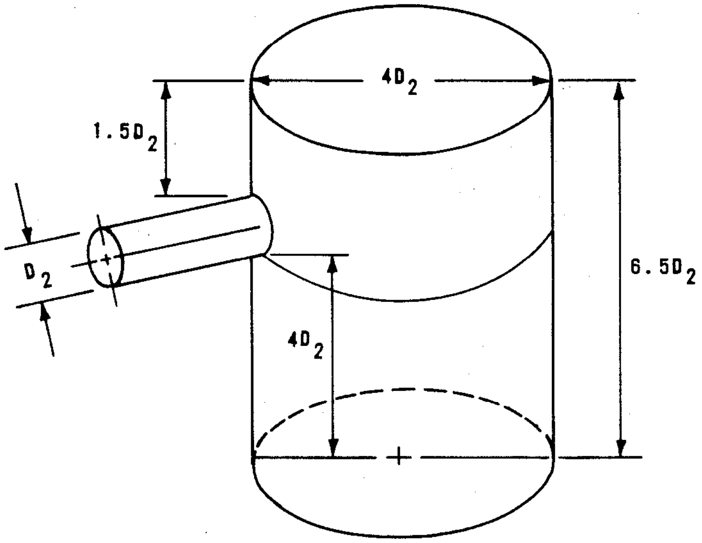

Figure 20. Recommended design.

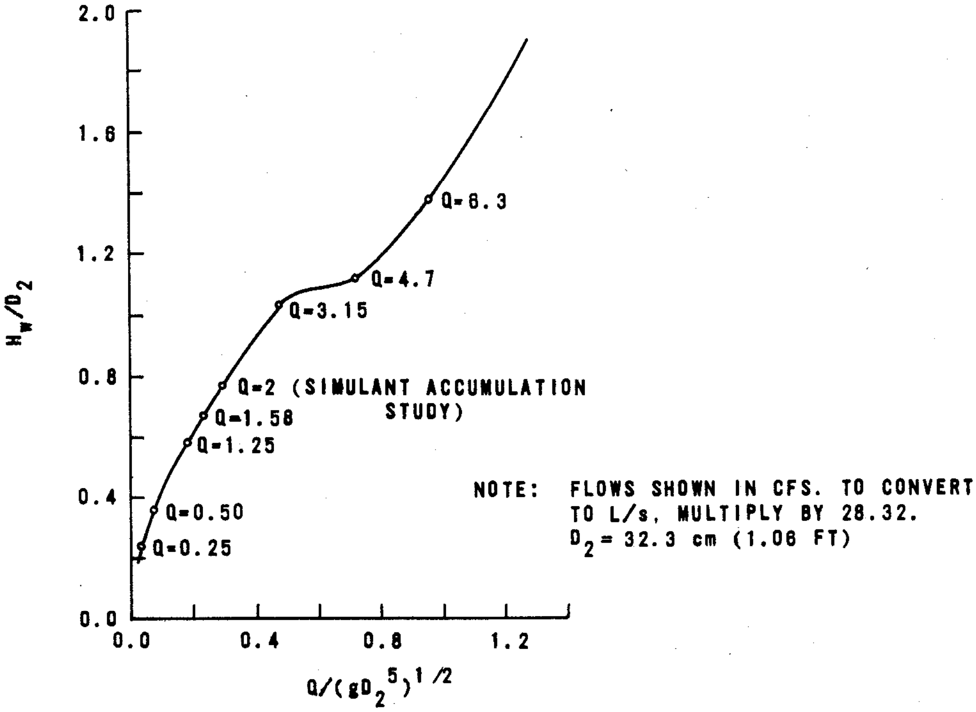

Figure 21. Discharge rating curve for recommended design.

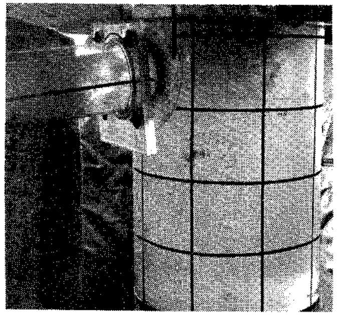

Photograph 26
Q = 6.30 cfs (100%) short tube control, plunging jet with macro eddy
$HW/D_2 = 1.37$ $Q/(gD_2^5)^{1/2} = 0.96$

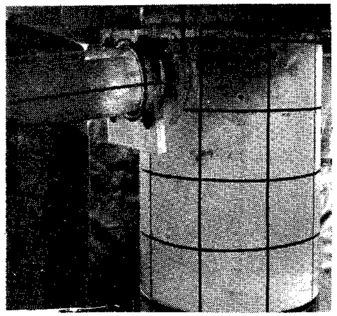

Photograph 27
Q = 4.70 cfs (75%) short tube control, slug flow, plunging jet with macro eddy
$HW/D_2 = 1.11$ $Q/(gD_2^5)^{1/2} = 0.72$

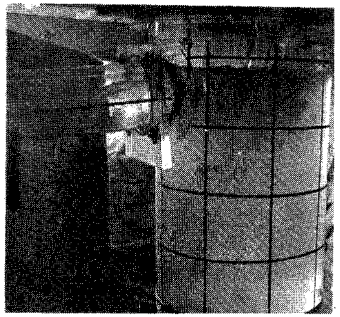

Photograph 28
Q = 3.15 cfs (50%) orifice control plunging jet with macro eddy
$HW/D_2 = 1.02$ $Q/(gD_2^5)^{1/2} = 0.48$

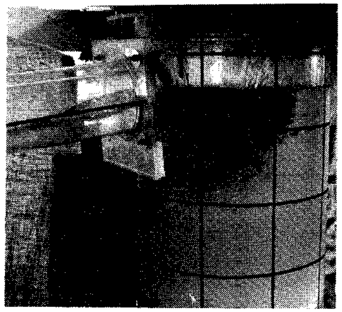

Photograph 29
Q = 1.58 (25%) weir control, diving jet
$HW/D_2 = 0.66$ $Q/(gD_2^5)^{1/2} = 0.24$

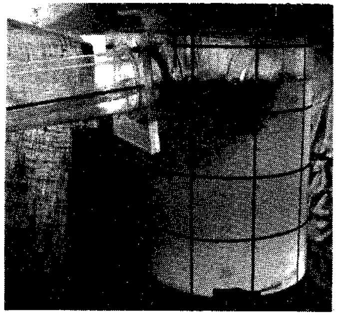

Photograph 30
Q = 1.25 cfs (20%) weir control, dissipating jet
$HW/D_2 = 0.57$ $Q/(gD_2^5)^{1/2} = 0.18$

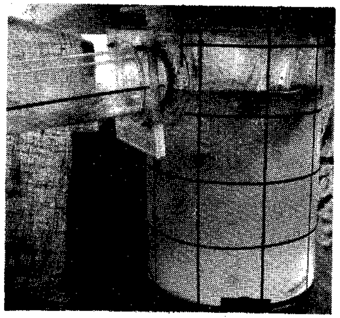

Photograph 31
Q = 0.50 cfs (8.00%) weir control dissipating jet
$HW/D_2 = 0.38$ $Q/(gD_2^5)^{1/2} = 0.076$

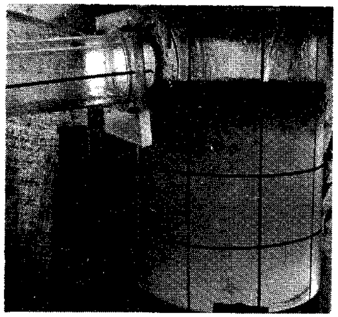

Photograph 32
Q = 0.25 cfs (4.00%) weir control dissipating jet
$HW/D_2 = 0.24$ $Q/(gD_2^5)^{1/2} = 0.038$

$D_1 = 4.01$ ft; $D_2 = 1.06$ ft
$H_1 = 6.69$ ft; $H_2 = 4.00$ ft
$H_3 = 1.50$ ft; $D_1/D_2 = 3.78$
$H_1/D_2 = 6.30$; $H_2/D_2 = 3.77$
$H_3/D_2 = 1.42$

Control and Flow Conditions
Recommended Basin

Figure 22. Photographic record - recommended basin.

Sediment Capture--

A graded solids simulant, shown in Figure 11, was used to test the sediment capture characteristics of the recommended design as a function of flow, particle size, and accumulated deposits in the storage basin. For each test, a batch of simulant was prepared with the following size-weight distribution. Double batches were used in the accumulation test.

Size range, mm	Weight, g (lb)
>2.0	364 (0.8)
0.84 to 2.0	909 (2.0)
0.25 to 0.84	1,364 (3.0)
0.10 to 0.25	909 (2.0)
Total	3,546 (7.8)

With the exception of the accumulation test, the basin and setup were cleaned between each run. The results of flow variation on sediment capture in clean basins are shown in Table 21 and Figures 23 and 24. While there is a loss in efficiency at higher flows, a well-designed basin is surprisingly tolerant of wide flow variations *with respect to heavy solids removal.* For example, a twenty-fivefold increase in flow reduced the net removal efficiency only from 90 to 35 percent. However, in the small particle size range (the most critical range with respect to pollution load), the dropoff was much more dramatic: a sixfold increase in flow reduced the removal efficiency from 68 to 14 percent. These results must be interpreted only as trends, since replicate runs were not conducted and the specific gravity for all size ranges was held at 2.65.

TABLE 21. PERCENT SEDIMENT RETAINED IN BASIN VERSUS DISCHARGE

Size of simulant, mm	Q, cfs[a]						
	6.3	4.7	3.15	1.58	1.25	0.50	0.25
>2.0	75.20	83.24	90.17	96.12	96.34	98.98	99.44
0.84 to 2.0	50.03	57.93	78.62	93.19	96.00	98.88	99.33
0.25 to 0.84	33.04	26.41	56.85	72.51	81.18	91.54	97.46
0.10 to 0.25	4.64	6.37	7.67	14.72	32.23	45.24	68.60
0.10 to 2.0	34.44	35.18	53.24	65.42	73.98	82.31	90.74

a. L/s = cfs x 28.32.

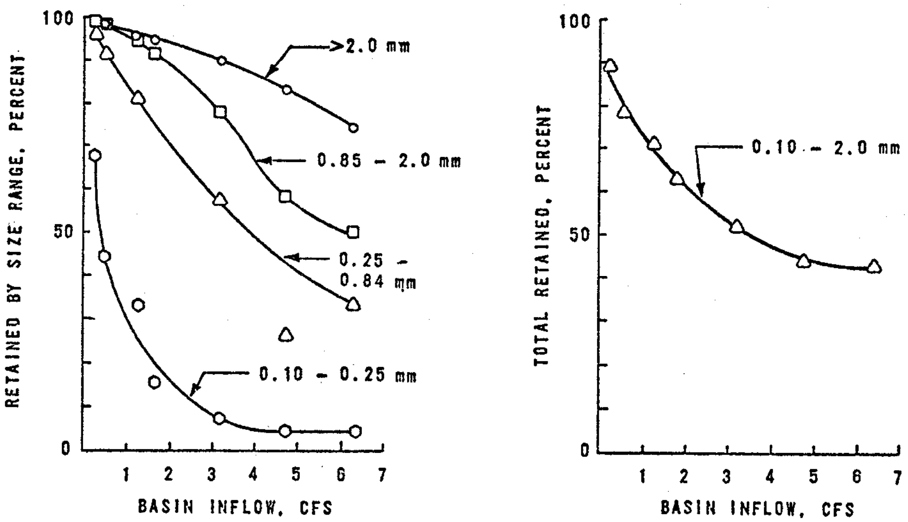

Figure 23. Sediment capture versus discharge.

In the final test, the simulant was allowed to accumulate in the basin through a series of runs at a constant flowrate. The results, as shown in Table 22 and Figures 25, 26, and 27, show the removal efficiencies to be relatively unaffected until a breakthrough point is reached, at which time they become erratic and even negative. This breakthrough in the experimental test occurred when the storage basin was filled to just over one-half its depth. The cumulative percent retained by particle size at the point of breakthrough is shown in Table 23.

TABLE 22. SEDIMENT ACCUMULATION[a]

Event	Cumulative weight, lb[b]	Depth, as fraction of H_2[c]
1	11.4	.04
2	22.3	.08
3	33.3	.12
4	44.1	.15
5	55.1	.19
6	66.3	.23
7	77.6	.27
8	88.2	.30
9	98.6	.34
10	108.4	.37
11	116.9	.40
12	126.1	.43
13	135.1	.46
14	143.4	.49
15	151.3	.52
16	159.1	.55
17	162.4	.56
18	167.9	.58
19	170.4	.59
20	167.0	.57

a. Q = 56.6 L/s (2.0 cfs).

b. g = lb x 454.

c. H_2 = distance from floor to invert of outlet pipe.

Photograph 33
Q = 6.30 cfs (100%) short tube control, plunging jet with macro eddy
$HW/D_2 = 1.39 \quad Q/(gD_2^5)^{1/2} = 0.96$

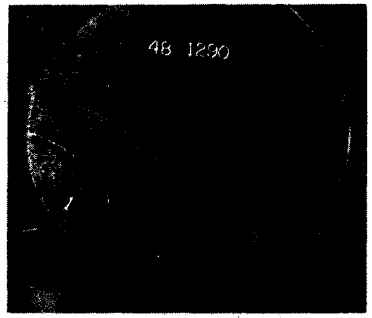

Photograph 34
Q = 4.70 cfs (75%) short tube control, slug flow, plunging jet with macro eddy
$HW/D_2 = 1.11 \quad Q/(gD_2^5)^{1/2} = 0.72$

Photograph 35
Q = 3.15 cfs (50%) orifice control, plunging jet with macro eddy
$Hw/D_2 = 1.02 \quad Q/(gD_2^5)^{1/2} = 0.48$

Photograph 36
Q = 1.58 cfs (25%) weir control, diving jet
$Hw/D_2 = 0.69 \quad Q/(gD_2^5)^{1/2} = 0.24$

Photograph 37
Q = 1.25 cfs (20%) weir control, dissipating jet
$HW/D_2 = 0.57 \quad Q/(gD_2^5)^{1/2} = 0.19$

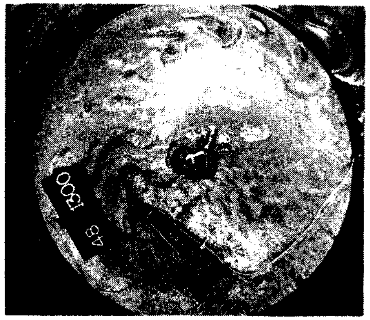

Photograph 38
Q = 0.50 cfs (8.00%) weir control, dissipating jet
$HW/D_2 = 0.43 \quad Q/(gD_2^5)^{1/2} = 0.076$

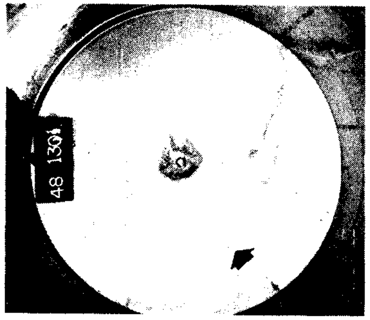

Photograph 39
Q = 0.25 cfs (4.00%) weir control, dissipating jet
$HW/D_2 = 0.29 \quad Q/(gD_2^5)^{1/2} = 0.038$

Note: Contour Elevation 1 = 0.23 ft prototype

Indicates direction of flow

Graded Simulant Retained in Catchbasin At Different Flow Rates

Figure 24. Photographic record - sediment capture versus discharge.

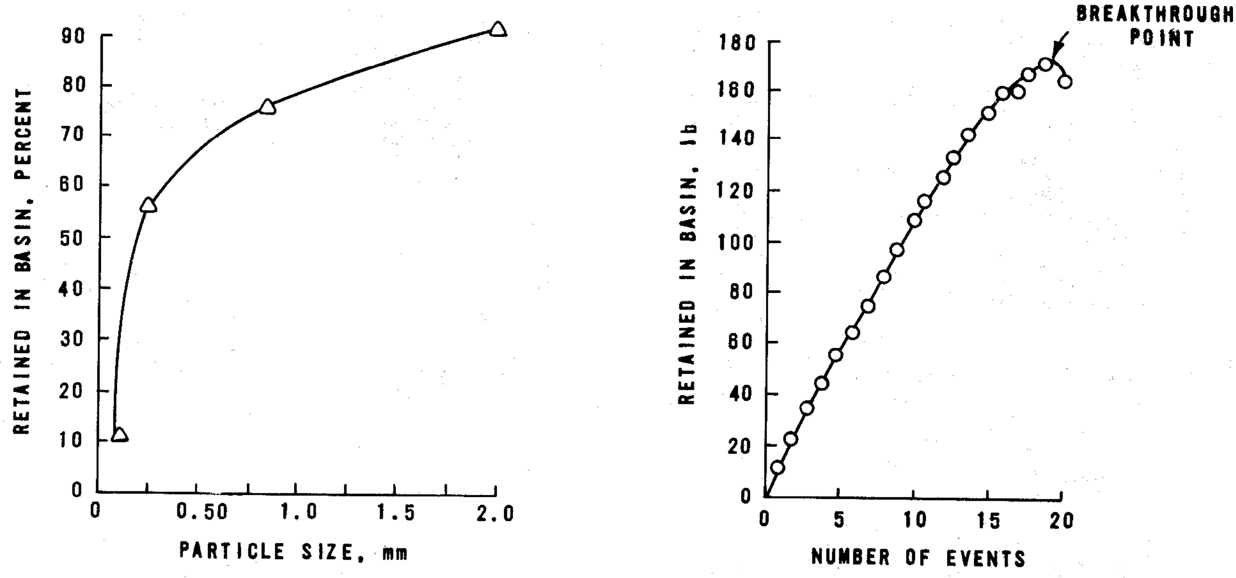

NOTE: 1 EVENT CORRESPONDS TO THE ADDITION OF 7,092 g (15.6 lb) GRADED SIMULANT. Q=56.6 L/s (2.0 cfs)

Figure 25. Sediment capture versus accumulation.

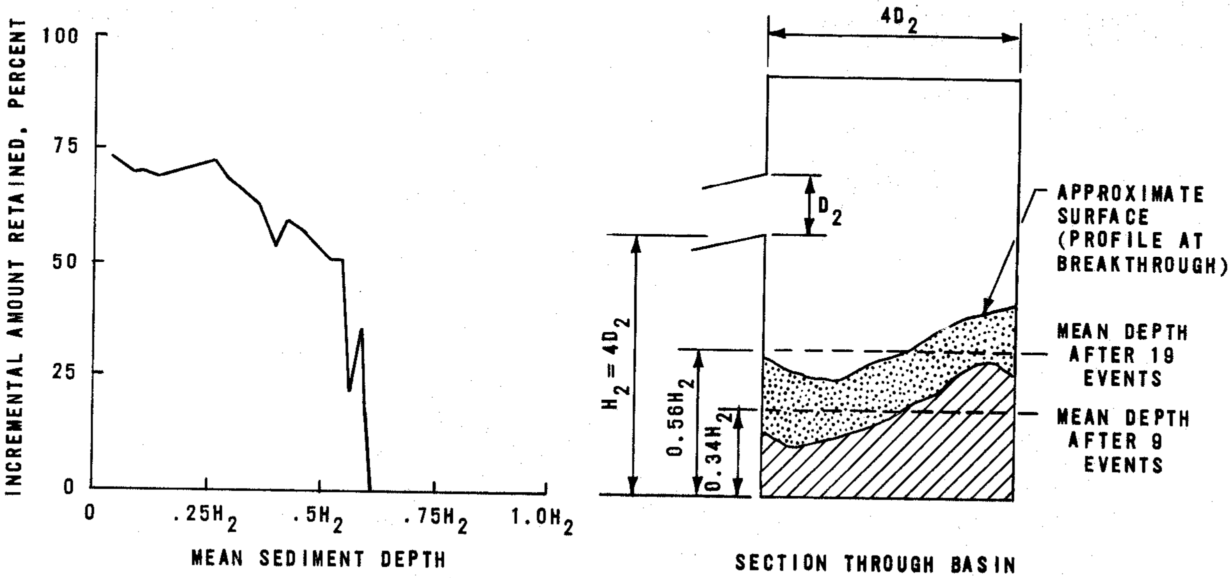

Figure 26. Sediment capture versus accumulated depth.

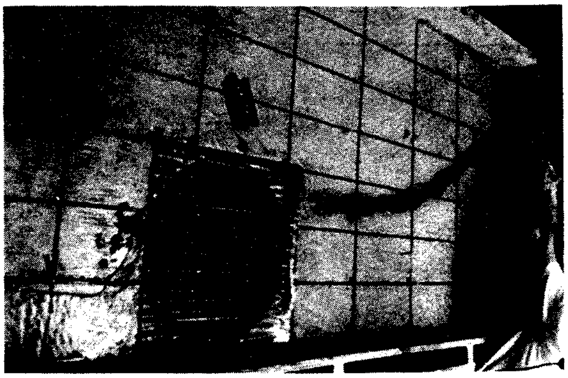

Photograph 40
Approach flow conditions during simulant accumulation study.

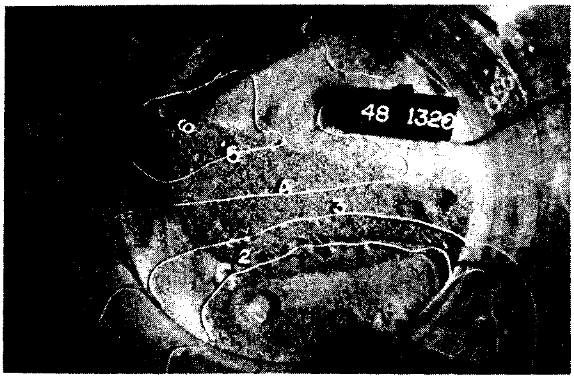

Photograph 41
Simulant accumulation after after 78 lb

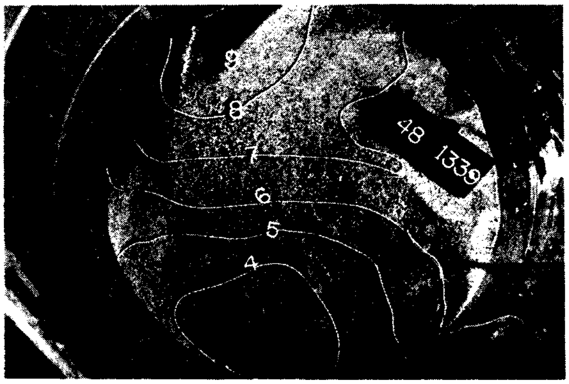

Photograph 42
Simulant accumulation after 140 lb

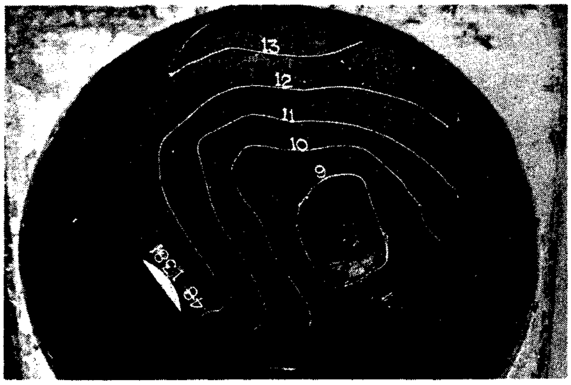

Photograph 43
Simulant accumulation after 312 lb

Graded Simulant retained in Catchbasin During Accumulation Study

Q = 2 cfs

Note: Contour Elevation Numerals correspond to the following:

13 = 2.95 ft	10 = 2.27 ft	7 = 1.59 ft	4 = 0.90 ft
12 = 2.72 ft	9 = 2.04 ft	6 = 1.36 ft	3 = 0.68 ft
11 = 2.49 ft	8 = 1.81 ft	5 = 1.13 ft	2 = 0.45 ft

Figure 27. Photographic record - sediment accumulation.

TABLE 23. AGGREGATE CAPTURE EFFICIENCIES AT BREAKTHROUGH

	Size, mm			
	2.0	0.84 to 2.0	0.25 to 0.84	0.10 to 0.25
Cumulative % retained at optimum event	90.11	75.43	47.77	10.0[a]

a. Estimated. Direct measurement impossible because of carryover of fines to sump and recycle system. 58.74% measured in trap basin and tank.

CONCLUSIONS

The following conclusions are drawn from the hydraulic model analysis:

1. Properly designed and maintained catchbasins can be very efficient in removing medium to very coarse sands from stormwater runoff. Further, the removals remain high over a wide range of flows and reduce to approximately 35 percent at maximum design inflow.

2. Removal efficiencies, as expected, are very sensitive to particle size and specific gravity. Under the test conditions examined, the removal of fine sands ranged from fair to poor with increasing flow. Removals of very fine sand and low specific gravity material (gilsonite) were negligible at 40 percent of maximum flow.

3. Storage basin depth is the primary control for performance; efficiencies improve with increasing depth.

4. The accumulation of sediment in catchbasins does not appear to impair solids removal efficiencies until 40 to 50 percent of the storage depth is filled. Beyond this depth, removals drop rapidly, even to the point of negative values (washout exceeds sedimentation).

5. Of the standard modifications tested, hoods or traps were found to increase the discharge head requirements significantly. In the higher flow ranges, increased scour currents were observed as the flow was diverted downward by the obstruction of the outlet. By comparison, curb openings or protrusions had negligible effect.